RHIC – Beam Energy Scan Program: Experimental Highlights

Bedanga Mohanty

Measurements at …

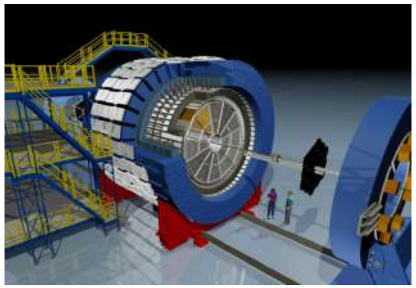

Outline:
- Heavy-ion collisions
- Motivation for RHIC BES program
- STAR detector for RHIC BES program
- Measurements from RHIC BES Program
  - Chemical freeze-out
  - Collectivity
  - Criticality
  - Chirality
- Summary and outlook (BES-phase-II)

4C's

Based only on published experimental results …..

Phase diagram of matter

Physical systems undergo phase transitions when external parameters such as the temperature (T) or a chemical potential (μ) are tuned.

Phase diagram of QED matter.

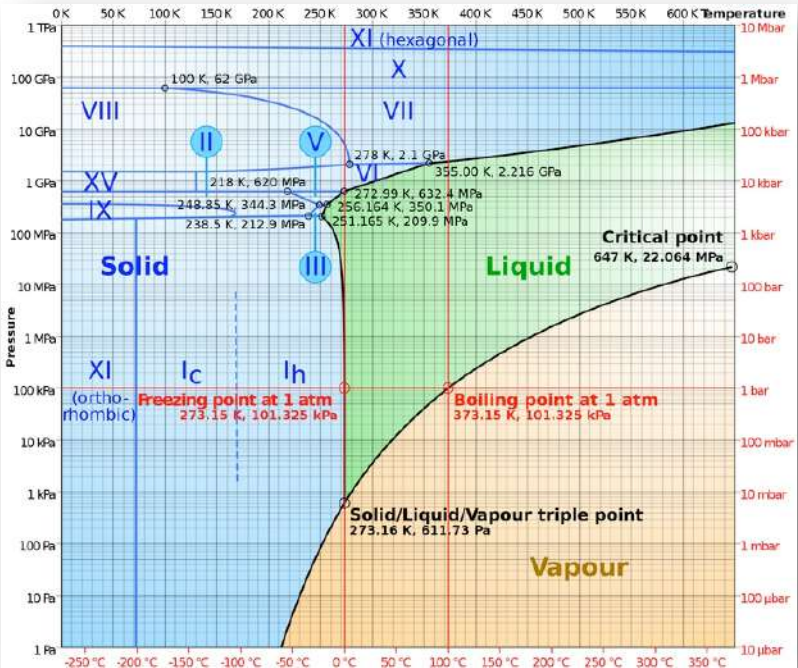

Wiki

Phase diagram of QCD matter.

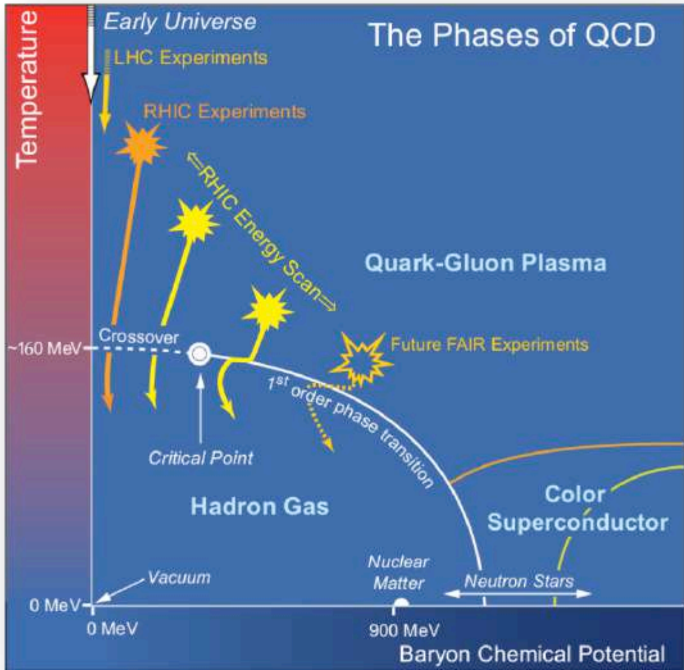

NSAC LRP 2007

Widely studied, precisely known, studied for many systems, and part of textbook.

Largely conjectured, unique, needs accelerators, goal to make it part of textbook.

Emergent properties of matter

Strongly correlated **QED** matter
Emergent property: strange metal

Strongly correlated **QCD** matter
Emergent property: perfect fluid

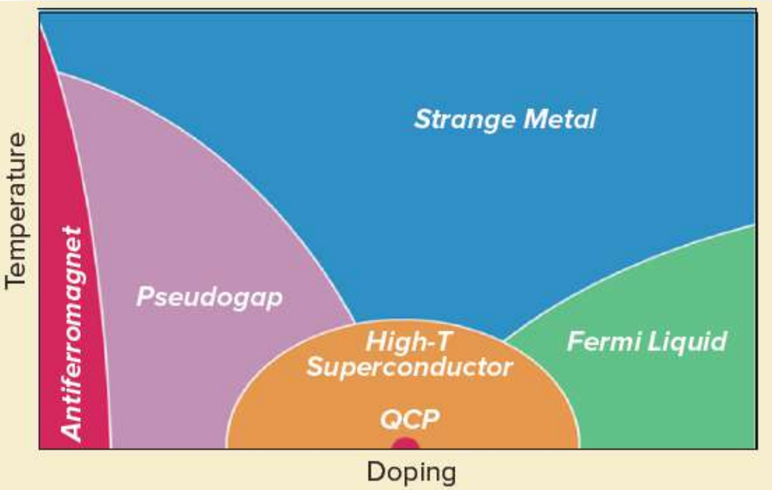

Condensed matter of QCD.

The Condensed matter physics of QCD, Krishna Rajagopal and Frank Wilczek e-Print: hep ph/ 0011333 [hep-ph]

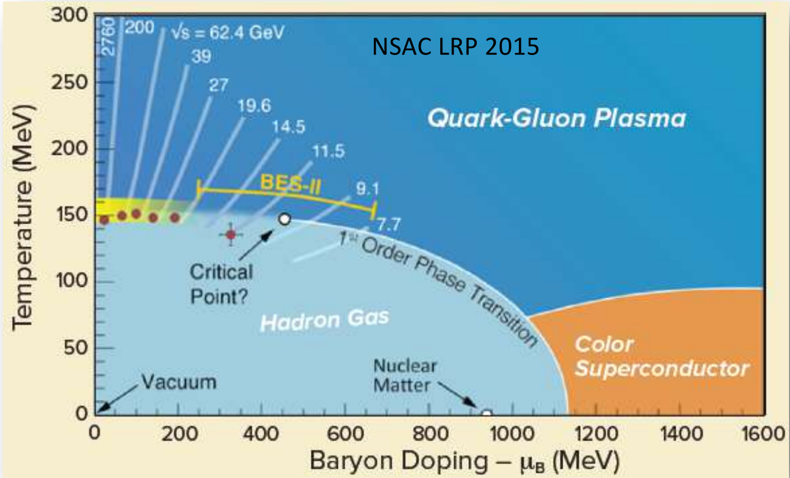

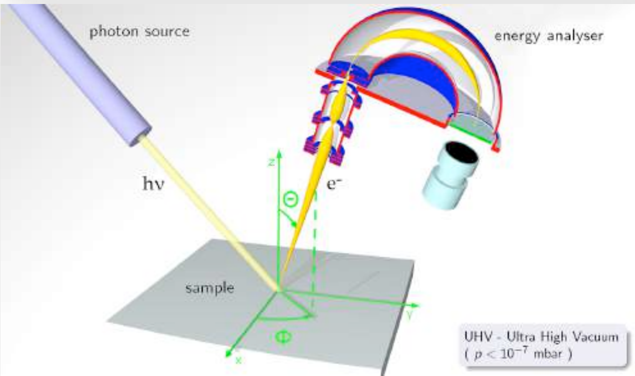

Experiments

Need to have experiments at various colliding energies - LHC, RHIC, FAIR, NICA and JPARC.

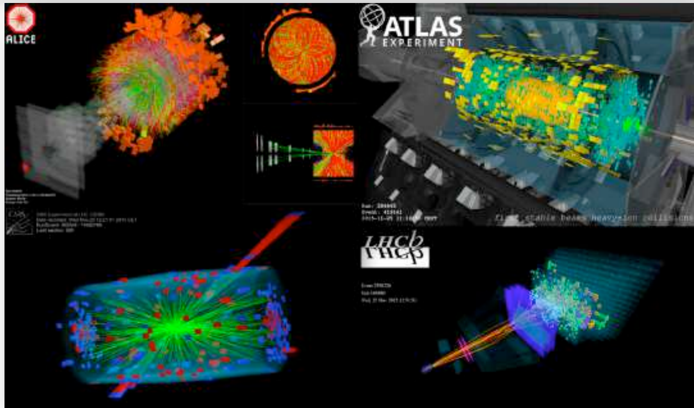

Heavy-ion collisions

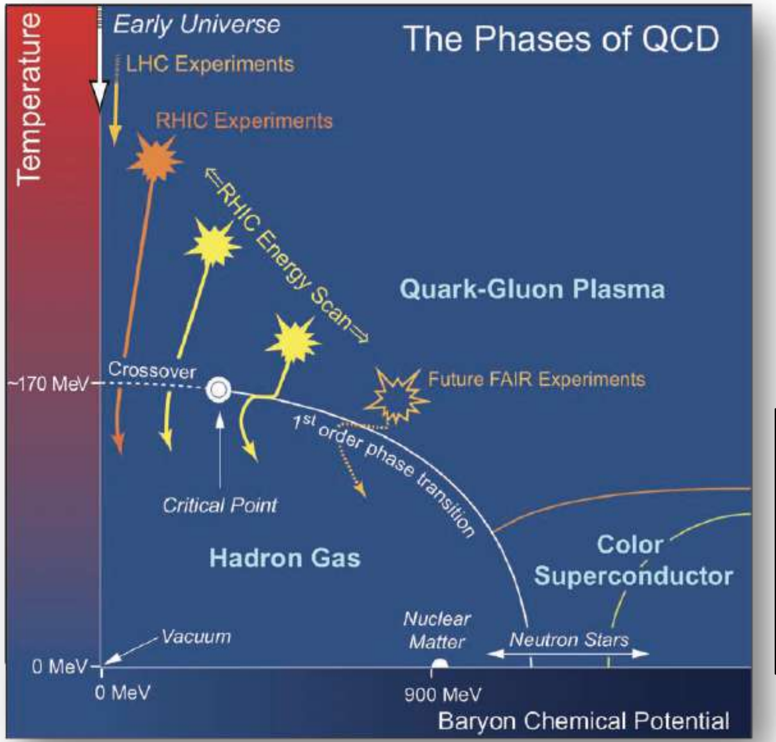

Fukushima, K. and Hatsuda, T., Rept. Prog. Phys. 74, 228 014001 (2011).
Bazavov, A. et al., Phys. Rev. D96, 074510 (2017); Phys. Rev. D95, 248 054504 (2017).

Varying beam energy varies the temperature and baryon chemical potential.

Goals: Study various phase structures:
(a) Quark gluon plasma and its properties.
(b) Nature of QCD transition.
(c) Search for critical point.
(d) Hadronic phase and its properties .

Conserved quantities:
Baryon number ~ μ_B
Electric charge ~ μ_Q ~ small
Strangeness ~ μ_S ~ small

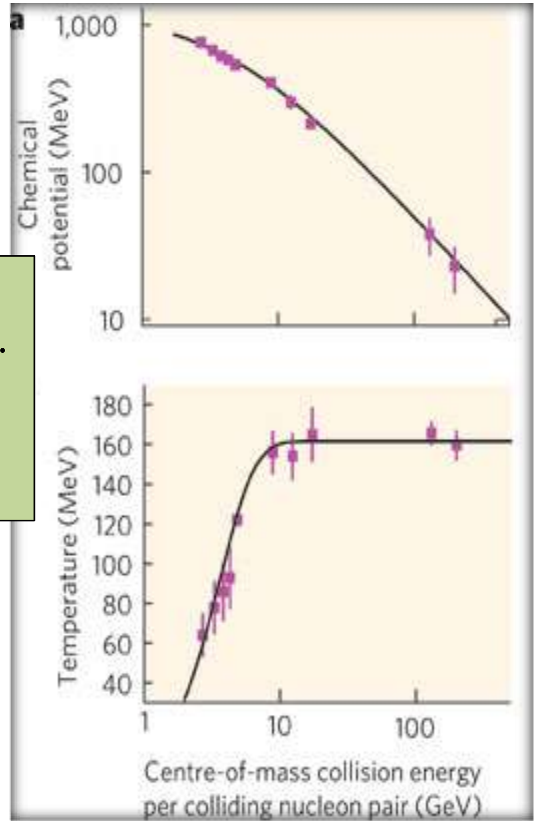

P. Braun-Munzinger, J. Stachel
Nature 448:302-309,2007

Heavy ion collisions (QGP)

Partonic energy-loss

RHIC top collision energy: 200 GeV/n

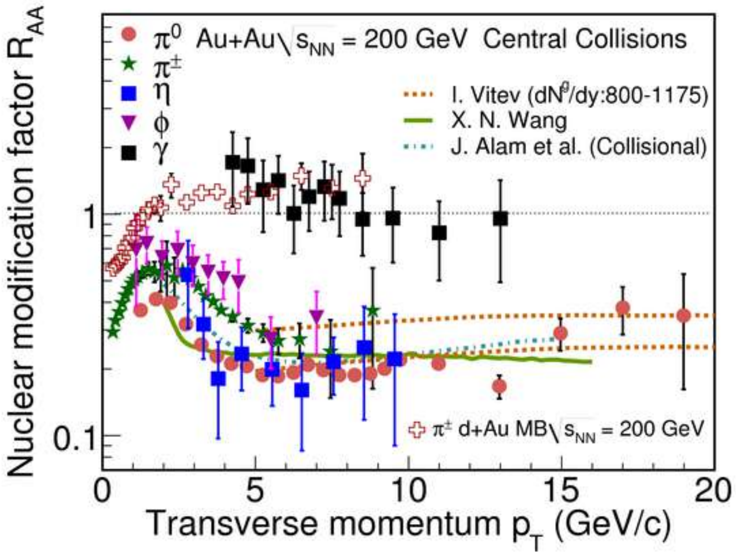

New J.Phys. 13 (2011) 065031

$$R_{AA}(p_T) = \frac{1}{T_{AA}} \frac{d^2N^{AA}/dp_T d\eta}{d^2\sigma^{NN}/dp_T d\eta}$$

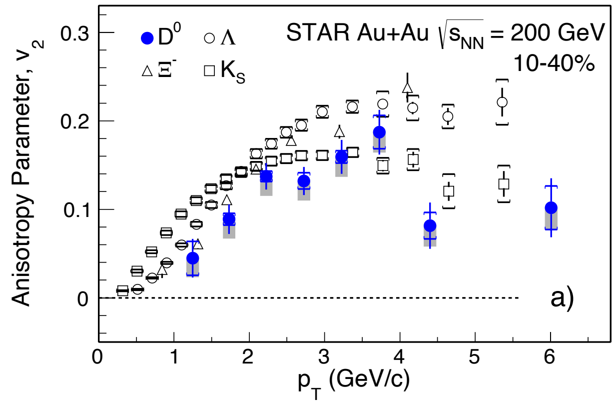

Partonic collectivity

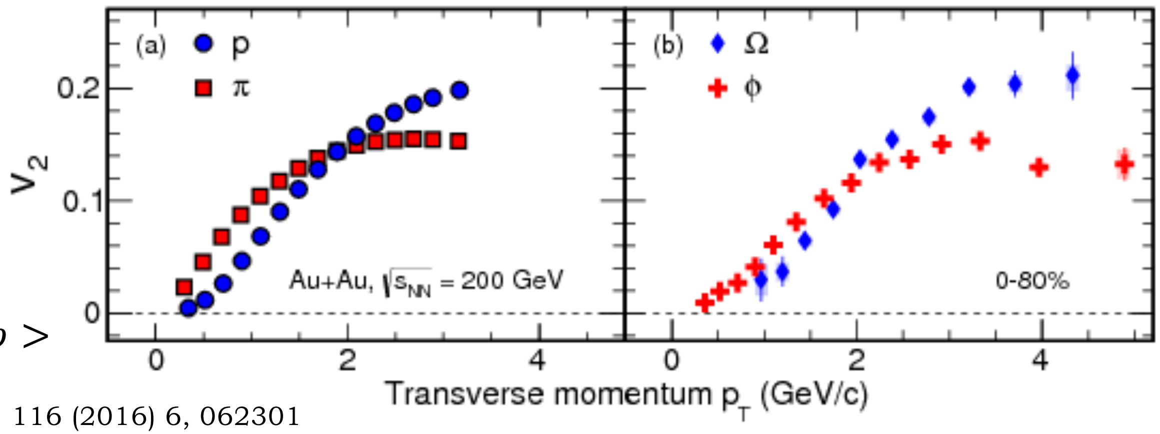

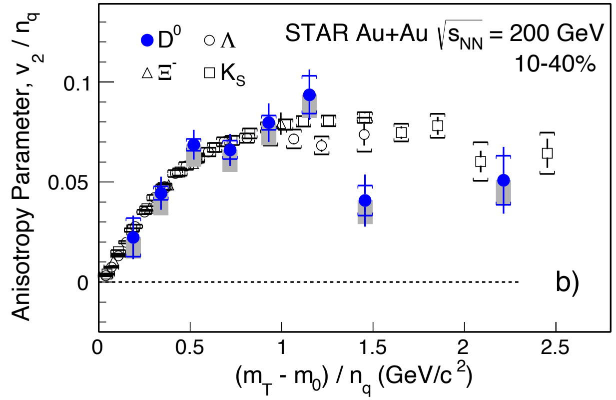

Elliptic flow

$v_2 = <\cos 2\varphi>$

Phys.Rev.Lett. 116 (2016) 6, 062301
Phys.Rev.Lett. 121 (2018) 3, 032301

Heavy ion collisions (QGP properties)

S. Bass et al.

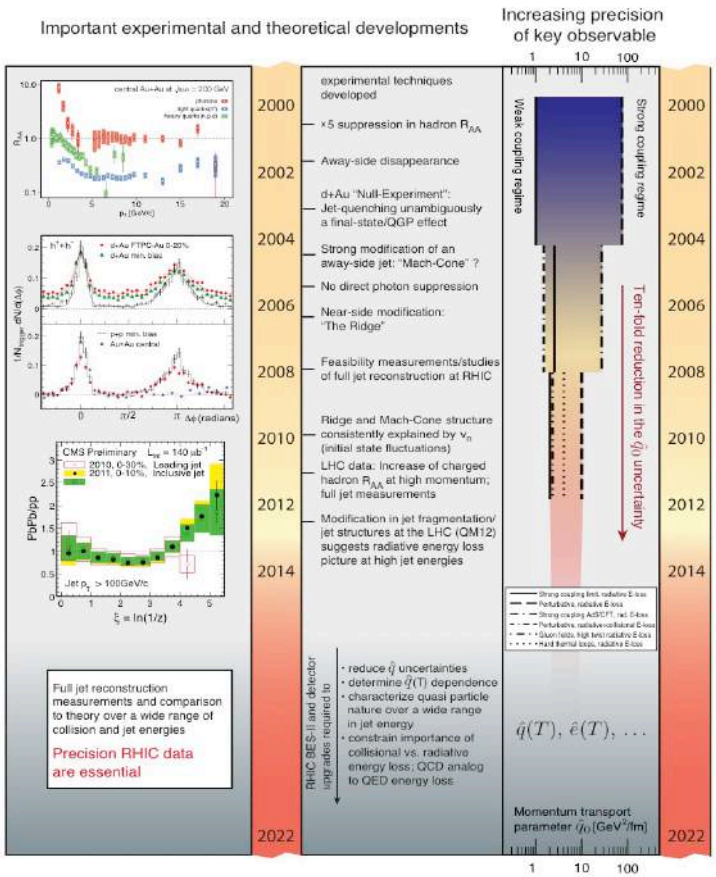

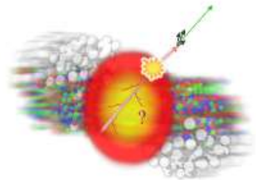

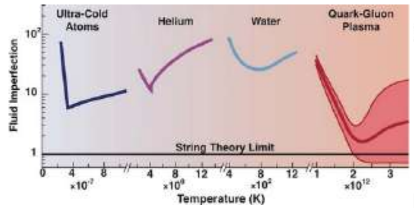

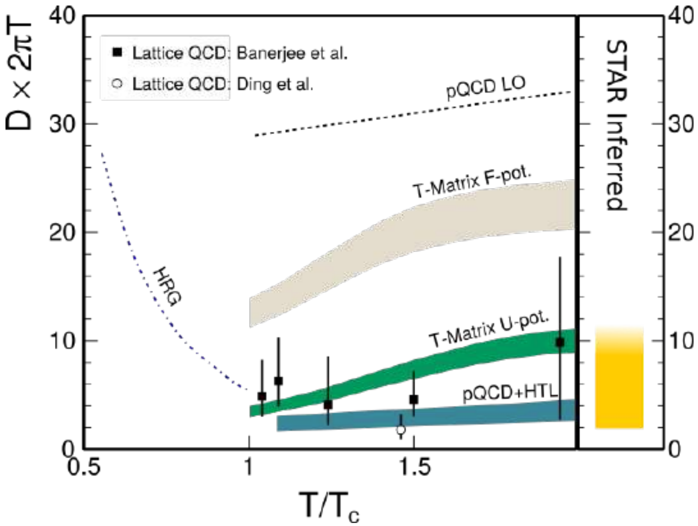

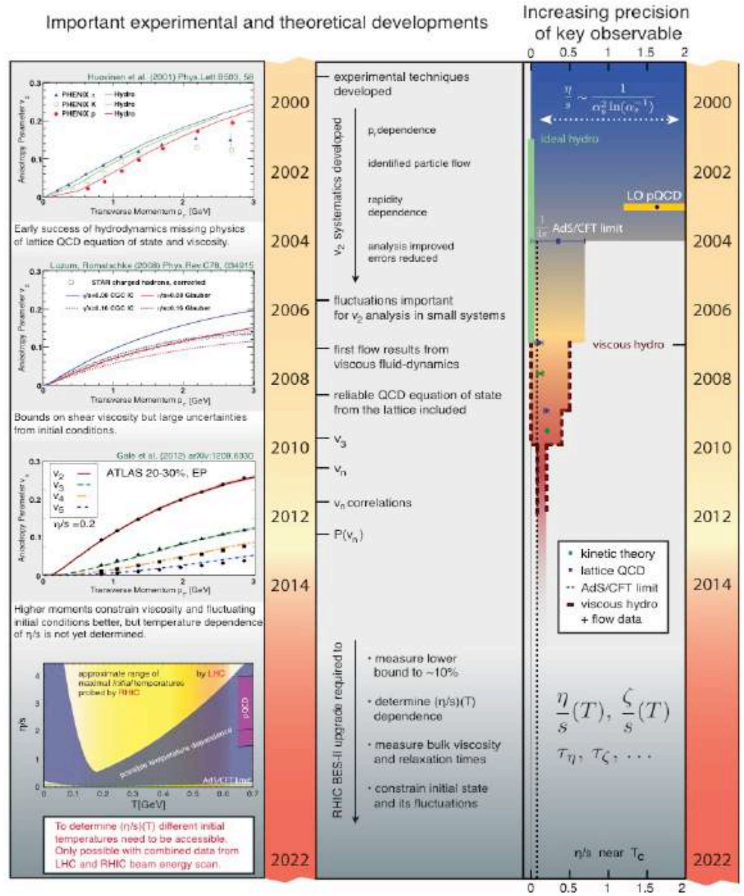

BES Program ➔ BEST

RHIC top collision energy: 200 GeV/n - ***Shear viscosity to entropy density*** ratio - *(1-2)/4π*, **stopping power** - *2-10 GeV²/fm* and **diffusion co-efficient** times 2πT - *1 – 10.*

Goals of RHIC BES-I program

	Collision Energies (GeV)	5	7.7	11.5	17.3	27	39
Section	Observables	Millions of Events Needed					
A1	n_q scaling $\pi/K/p/\Lambda$ $(m_T - m_0)/n < 2$GeV	8.5	**6**	**5**	**5**	**4.5**	**4.5**
A1	ϕ/Ω up to $p_T/n_q=2$ GeV/c		56	25	**18**	**13**	**12**
A2	R_{CP} up to $p_T \sim 4.5$ GeV/c (at 17.3) 5.5 (at 27) & 6 GeV/c (at 39)				**15**	**33**	**24**
A3	untriggered ridge correlations		27	13	**8**	**6**	**6**
A4	parity violation		**5**	**5**	**5**	**5**	**5**
B1	v_2 (up to ~1.5 GeV/c)	**0.3**	**0.2**	**0.1**	**0.1**	**0.1**	**0.1**
B1	v_1	0.5	**0.5**	**0.5**	**0.5**	**0.5**	**0.5**
B2	Azimuthally sensitive HBT	4	**4**	**3.5**	**3.5**	**3**	**3**
B3	PID fluctuations (K/π)	1	**1**	**1**	**1**	**1**	**1**
B3	net-proton kurtosis	5	**5**	**5**	**5**	**5**	**5**
B3	differential corr & fluct vs. centrality	5	**5**	**5**	**5**	**5**	**5**
B3	integrated p_T fluct (T fluct)						

SN0493 : Experimental Study of the QCD Phase Diagram & Search for the Critical Point: Selected Arguments for the Run-10 Beam Energy Scan : https://drupal.star.bnl.gov/STAR/starnotes/public/sn0493

(A) A search for turn-off of phenomena (QGP) already established at higher RHIC energies.
(B) A search for signatures of a phase transition and a critical point.

RHIC-BES test run @ 9.2 GeV

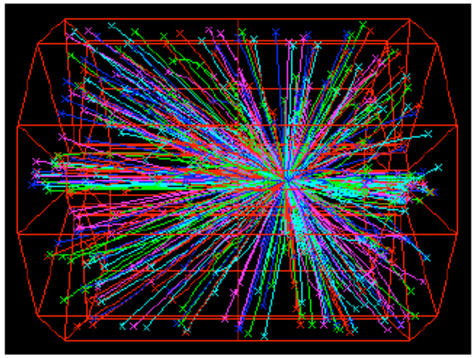

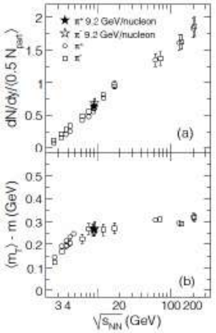

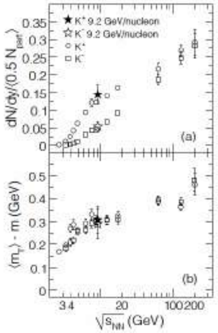

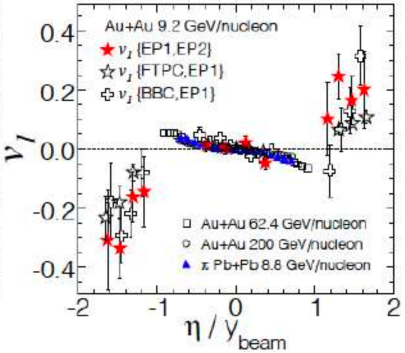

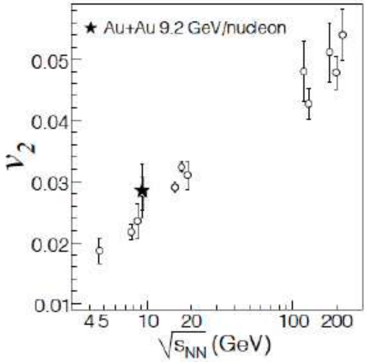

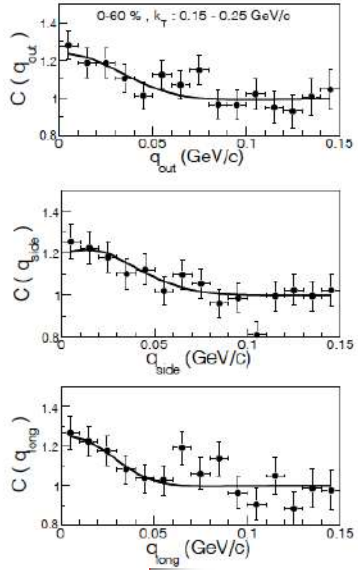

PHYSICAL REVIEW C **81**, 024911 (2010)

Identified particle production, azimuthal anisotropy, and interferometry measurements in Au + Au collisions at $\sqrt{s_{NN}} = 9.2$ GeV

We present the first measurements of identified hadron production, azimuthal anisotropy, and pion interferometry from Au + Au collisions below the nominal injection energy at the BNL Relativistic Heavy-Ion Collider (RHIC) facility. The data were collected using the large acceptance solenoidal tracker at RHIC (STAR) detector at $\sqrt{s_{NN}} = 9.2$ GeV from a test run of the collider in the year 2008. Midrapidity results on multiplicity density dN/dy in rapidity y, average transverse momentum $\langle p_T \rangle$, particle ratios, elliptic flow, and Hanbury-Brown–Twiss (HBT) radii are consistent with the corresponding results at similar $\sqrt{s_{NN}}$ from fixed-target experiments. Directed flow measurements are presented for both midrapidity and forward-rapidity regions. Furthermore the collision centrality dependence of identified particle dN/dy, $\langle p_T \rangle$, and particle ratios are discussed. These results also demonstrate that the capabilities of the STAR detector, although optimized for $\sqrt{s_{NN}} = 200$ GeV, are suitable for the proposed QCD critical-point search and exploration of the QCD phase diagram at RHIC.

3000 events

5 hours of data taking

2010 - 2017: BES-I at RHIC

$\sqrt{s_{NN}}$ (GeV)	Events (10^6)	Year	μ_B (MeV)	T_{CH} (MeV)
200	350	2010	25	166
62.4	67	2010	73	165
54.4	1200	2017	90	
39	39	2010	112	164
27	70	2011	156	162
19.6	36	2011	206	160
14.5	20	2014	264	156
11.5	12	2010	315	152
9.2	0.3	2008	355	140
7.7	4	2010	420	140

Goal to map the QCD phase diagram **$20 < \mu_B < 420$ MeV.**

STAR detector system @ RHIC

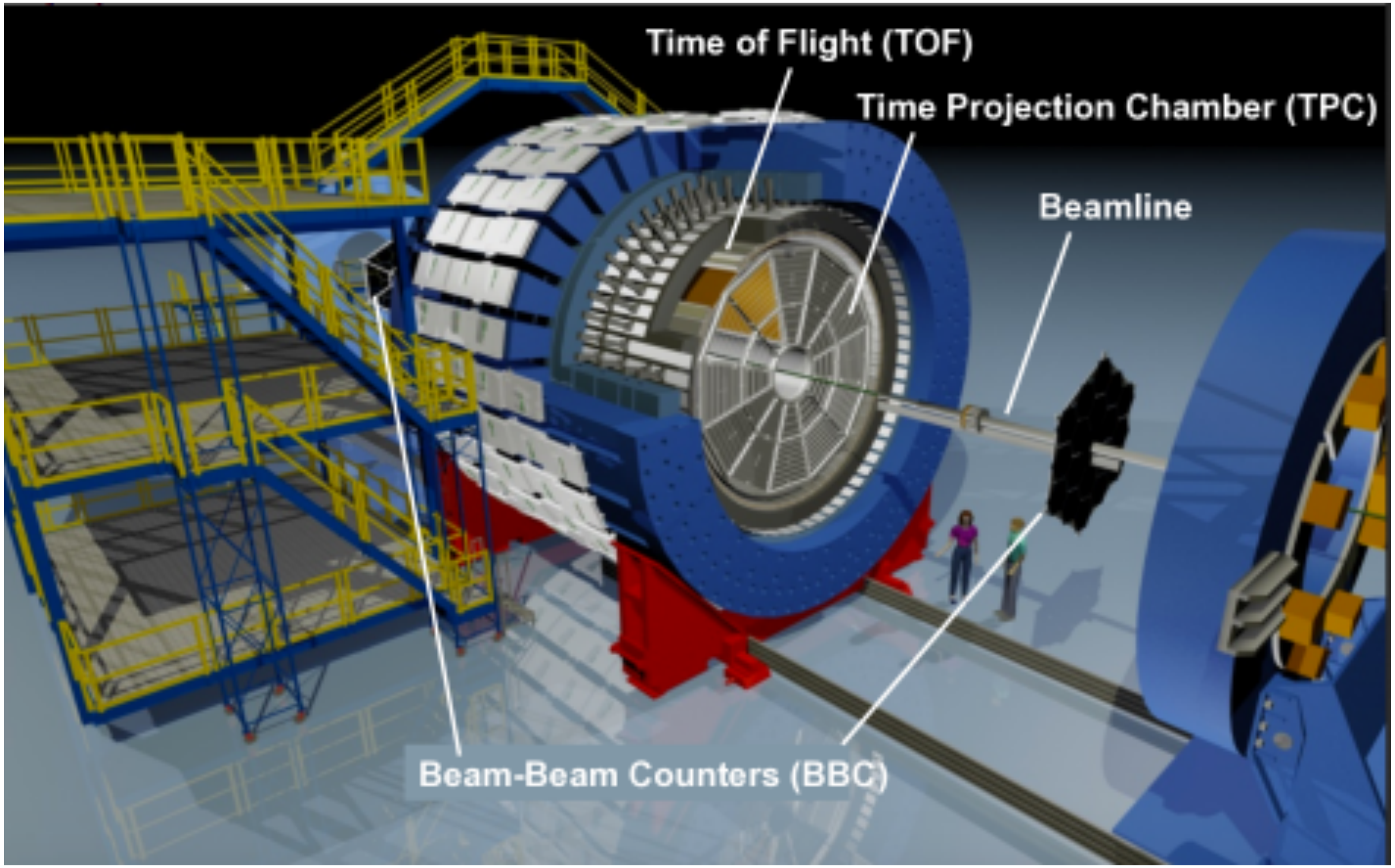

K. H. Ackermann et al. [STAR], Nucl. Instrum. Meth. A 499, 624-632 (2003) and Nucl. Instrum. Meth. A661, S110 (2012).

Uniform acceptance at mid-rapidity

Au+Au at *7.7 GeV*

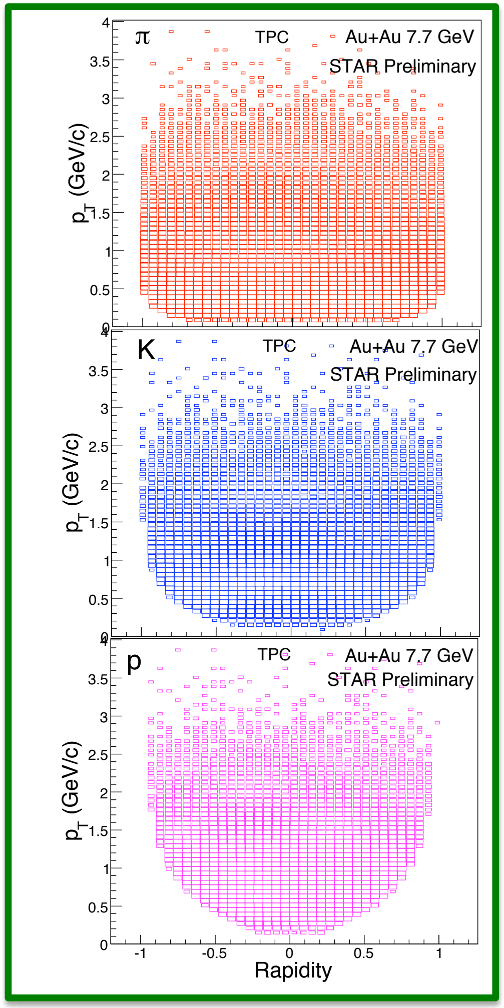

Au+Au at *39 GeV*

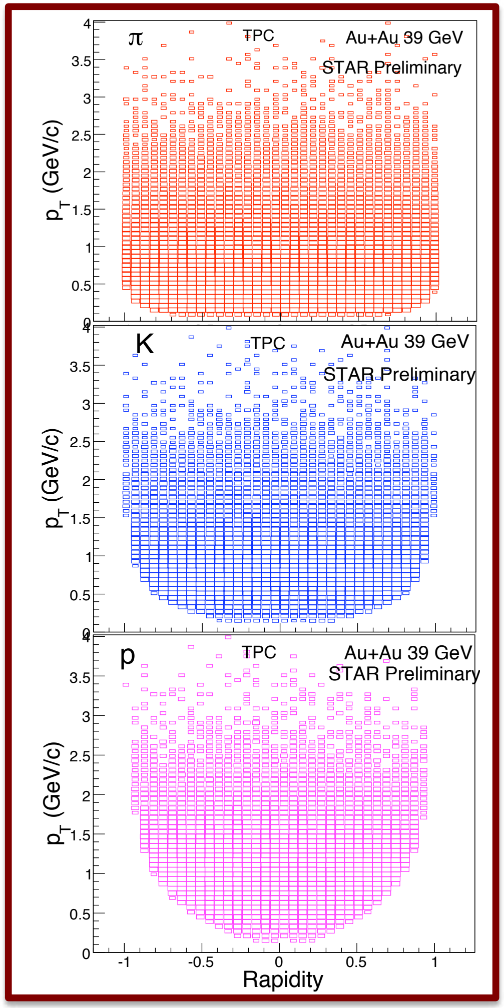

Au+Au at *200* GeV

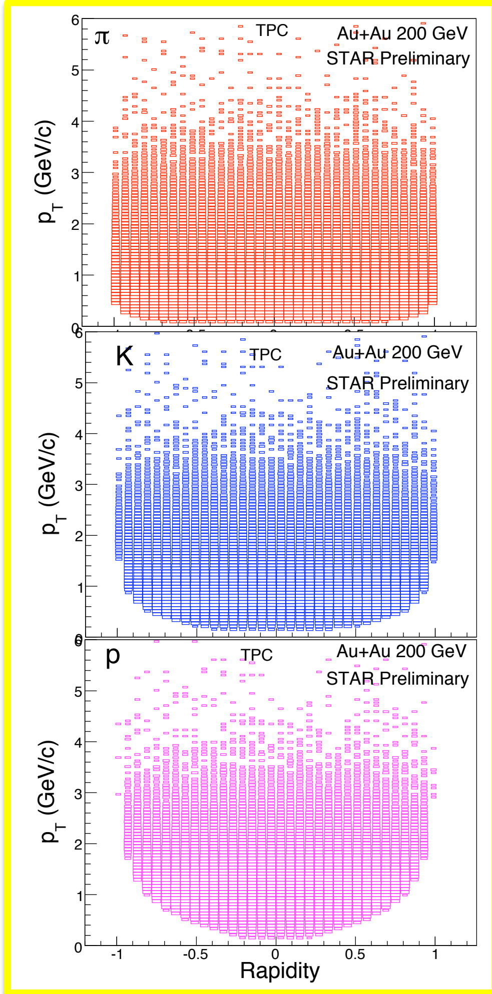

Particle identification

Time projection chamber

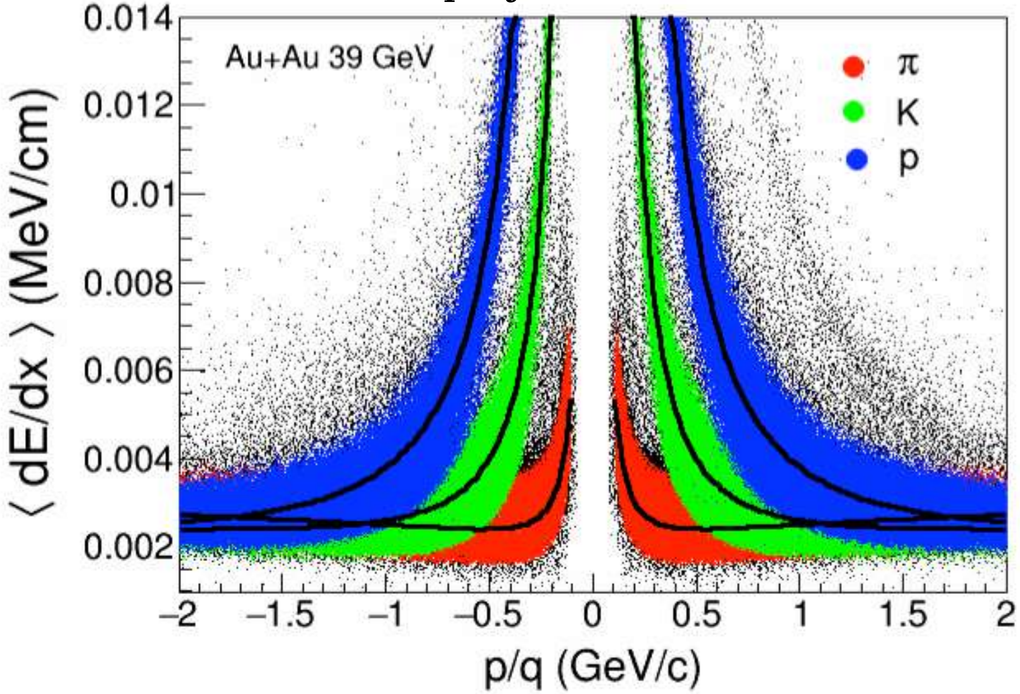

Time of flight detector

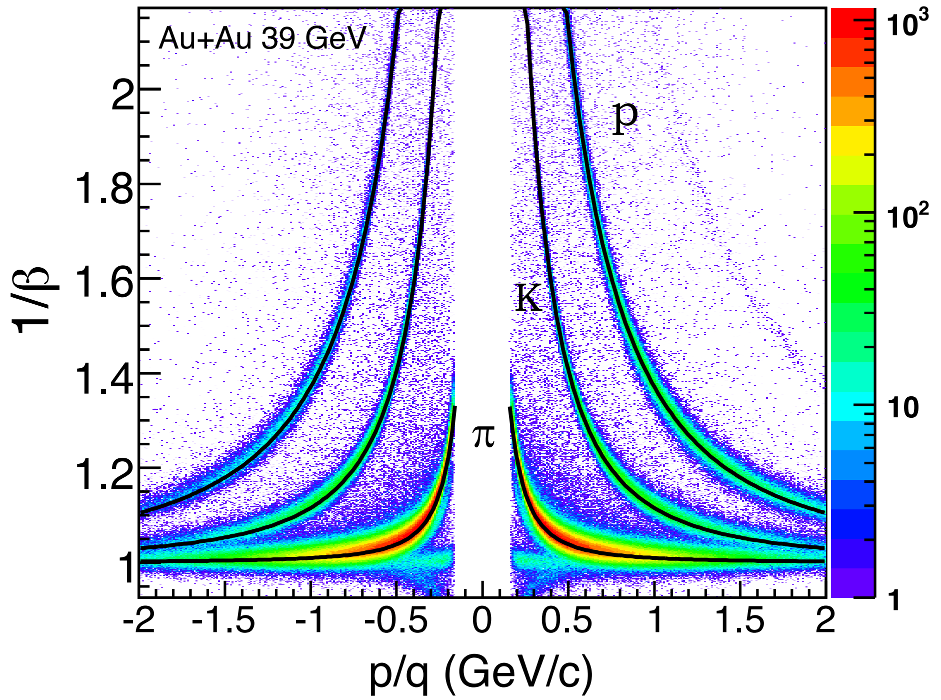

Ionization energy loss:

$- < dE/dx > \sim A / \beta^2$
$= A (1 + \mathbf{m^2} / p^2)$

Momentum $p = \gamma \beta m$

$m = [p (1 - \beta^2)^{1/2}] / \beta$

Time of flight:

$< \tau > = L / \beta$
$= L (1 + \mathbf{m^2} / p^2)^{1/2}$

STAR: Phys.Rev.C 96 (2017) 4, 044904

Chemical freeze-out related measurements

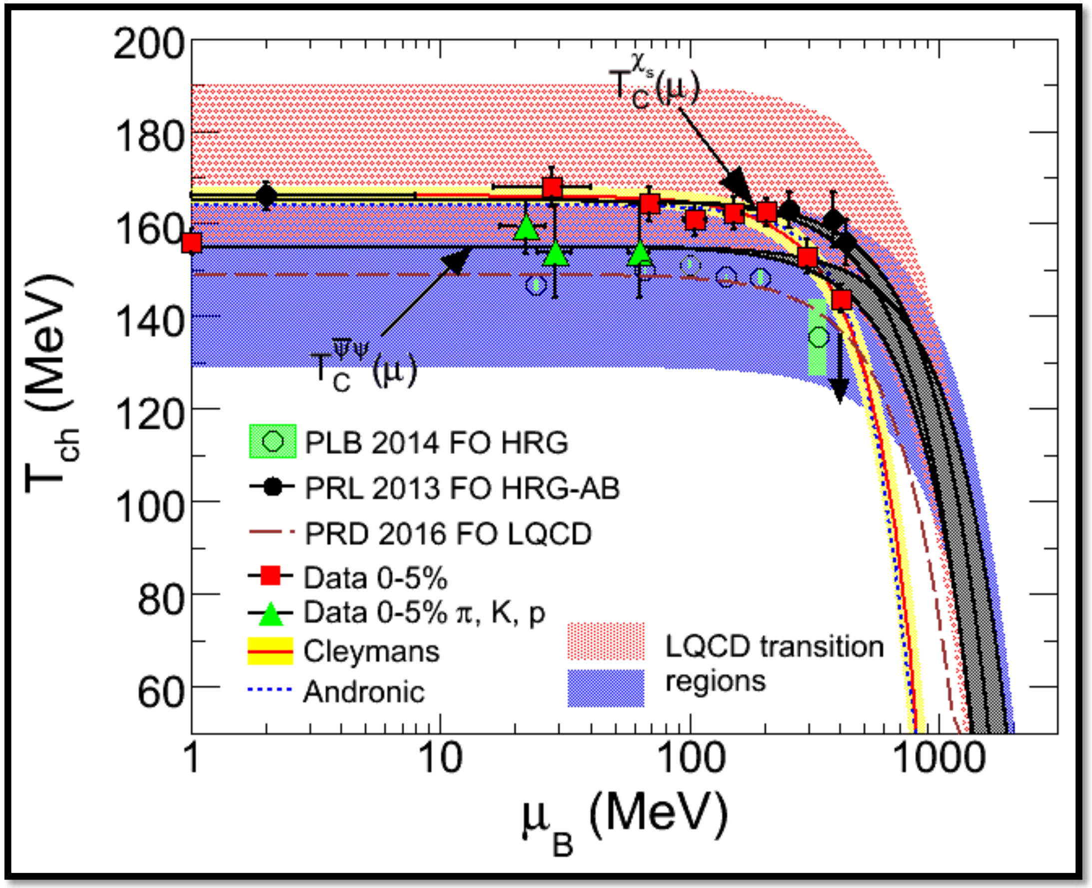

Based on STAR publications
Phys.Rev.C 96 (2017) 4, 044904
e-Print: 1906.03732 (to appear in PRC)
Phys.Rev.C 101 (2020) 2, 024905
Phys.Rev.C 99 (2019) 6, 064905

Editors' Suggestion

32 citations

Bulk properties of the medium produced in relativistic heavy-ion collisions from the beam energy scan program

L. Adamczyk *et al.* (STAR Collaboration)

Phys. Rev. C **96**, 044904 (2017) – Published 13 October 2017

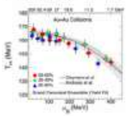

The beam-energy scan at RHIC aims to discover whether a critical point exists in the phase diagram of QCD. This paper reports on the most comprehensive measurement of single-particle spectra for a multitude of hadrons from the first run, taken with the STAR experiment. From these the authors infer the kinetic and chemical freeze-out temperatures and the baryon chemical potential as functions of beam energy and centrality. The results provide an opportunity for the beam-energy scan program at RHIC to enlarge the $(T, \mu B)$ region of the phase diagram to search for the QCD critical point.

Chemical freeze-out (data)

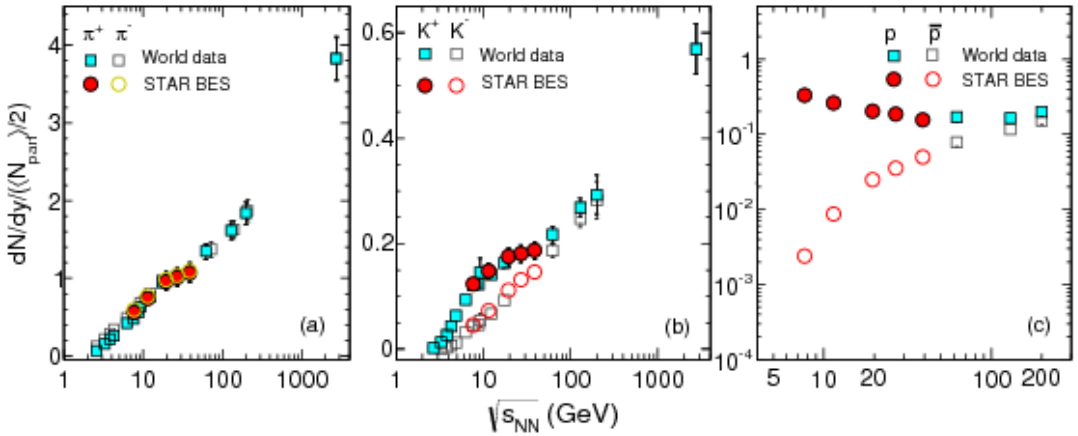

STAR: Phys.Rev.C 96 (2017) 4, 044904

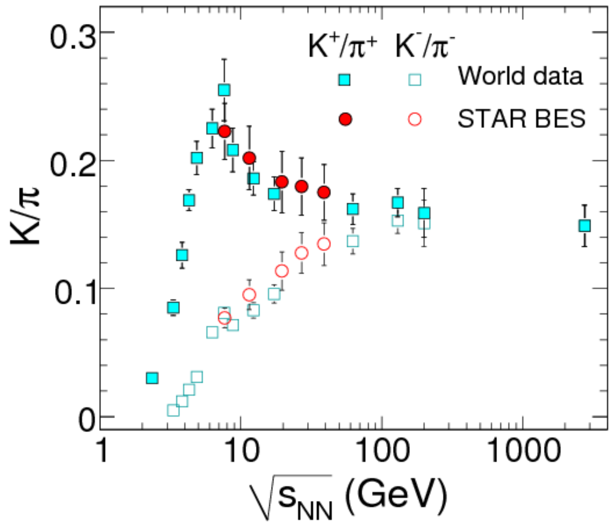

Particle yields, used to obtain the chemical freeze-out properties.

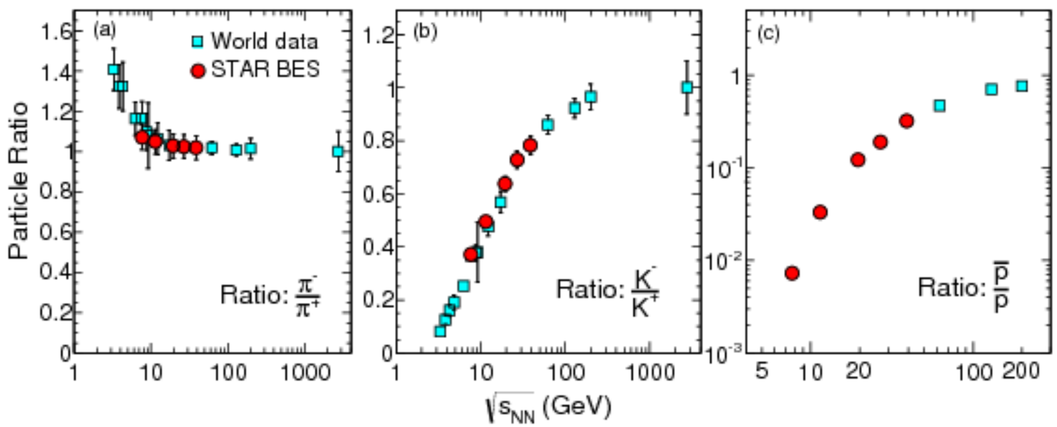

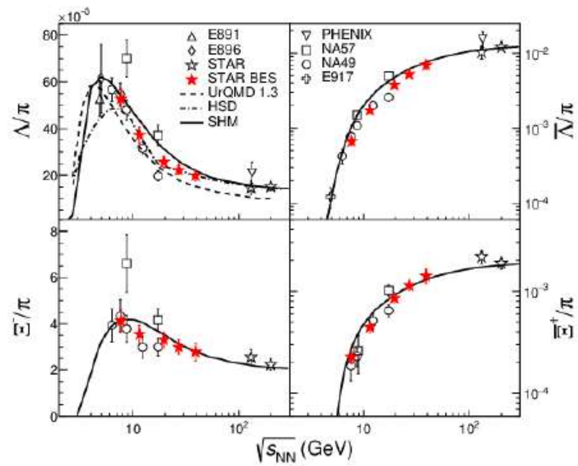

STAR: 1906.03732 [nucl-ex] To appear in PRC.

Chemical freeze-out dynamics (model)

Definition:
Inelastic collisions ceases
Chemical composition or
Particle ratios get fixed

Statistical Thermal Model

$$\ln Z^{GC}(T, V, \{\mu_i\}) = \sum_{\text{species i}} \frac{g_i V}{(2\pi)^3} \int d^3p \ln(1 \pm e^{-\beta(E_i - \mu_i)})^{\pm 1}$$

Particle Abundances: Grand Canonical Ensemble

$$N_i^{GC} = T \frac{\partial \ln Z^{GC}}{\partial \mu_i} = \frac{g_i V}{2\pi^2} \sum_{k=1}^{\infty} (\mp 1)^{k+1} \frac{m_i^2 T}{k} K_2\left(\frac{k m_i}{T}\right) \times e^{\beta k \mu_i}$$

Model Features:

- ❑ Assumes non-interacting hadrons and resonances
- ❑ Assumes thermodynamically equilibrium system
- ❑ Ensembles : Grand Canonical - average conservation of B, S, and Q
  Strangeness Canonical - exact conservation of S
  Canonical - exact conservation of B, S, and Q

Dynamics Characterized by:
Temperature T_{ch} and baryon chemical potential μ_B

Chemical freeze-out: data vs. model

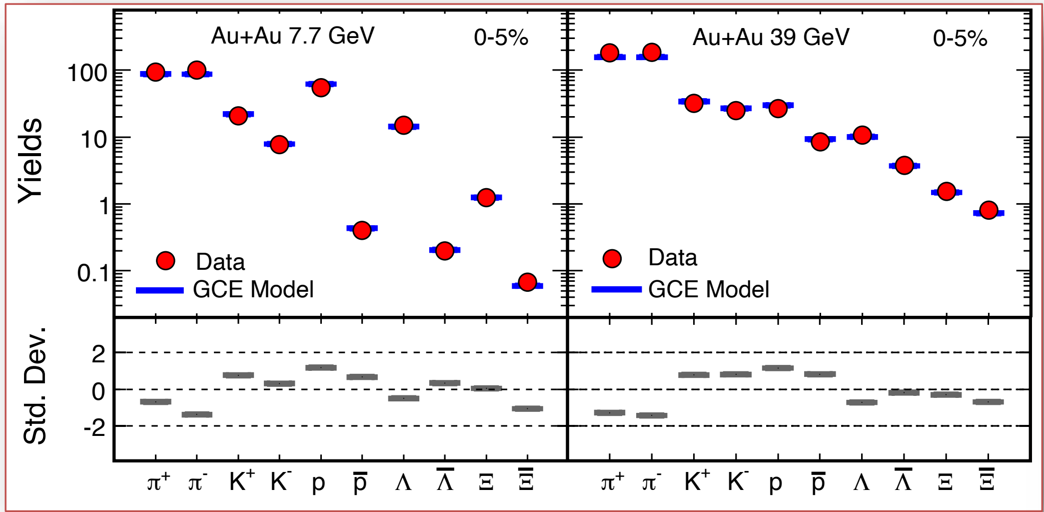

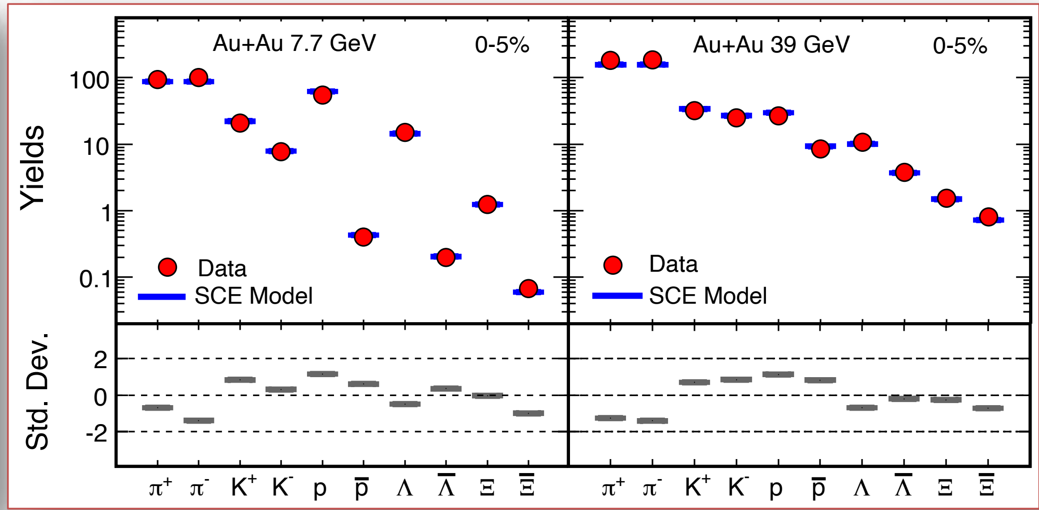

Fits to particle yields using a statistical thermal model with grand canonical and strangeness canonical model.

STAR: Phys.Rev.C 96 (2017) 4, 044904

Chemical freeze-out (hadrons)

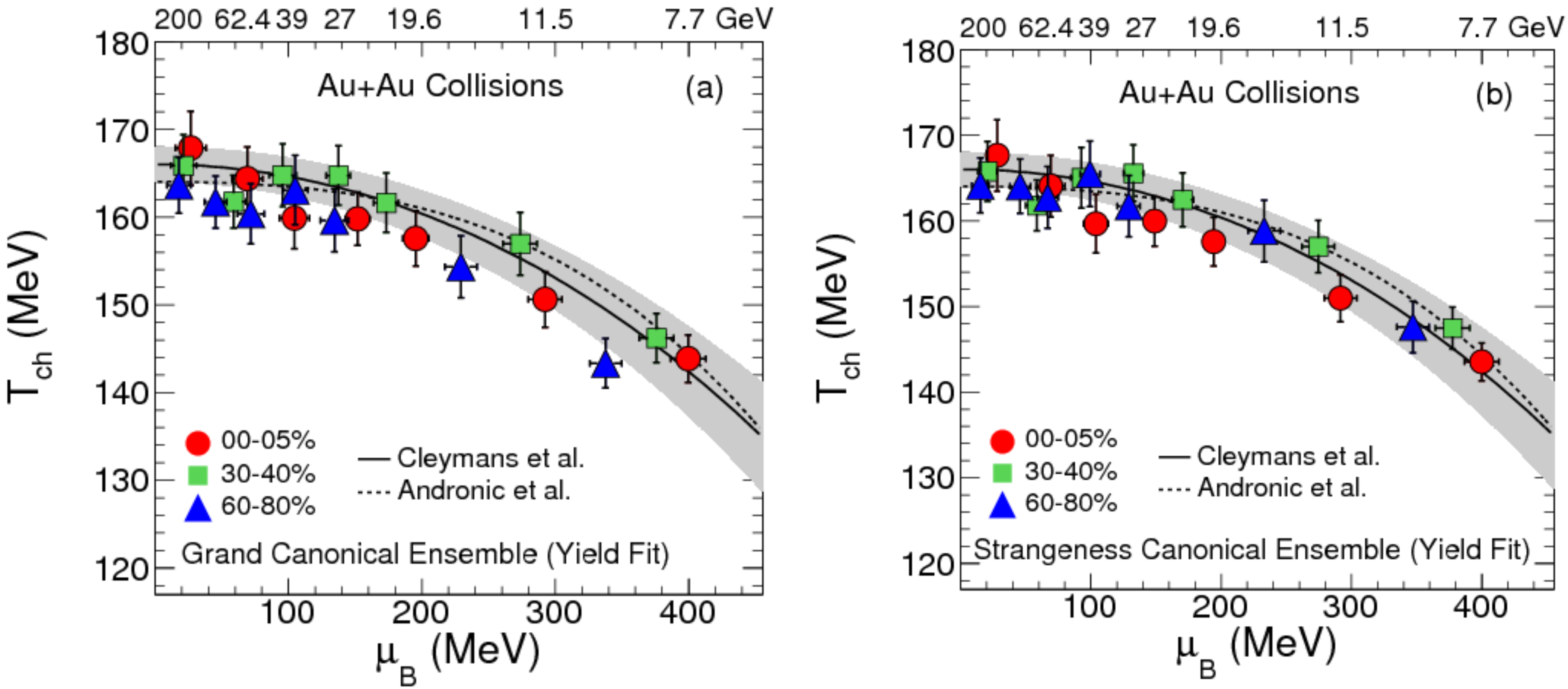

STAR: Phys.Rev.C 96 (2017) 4, 044904

Chemical freeze-out (nuclei)

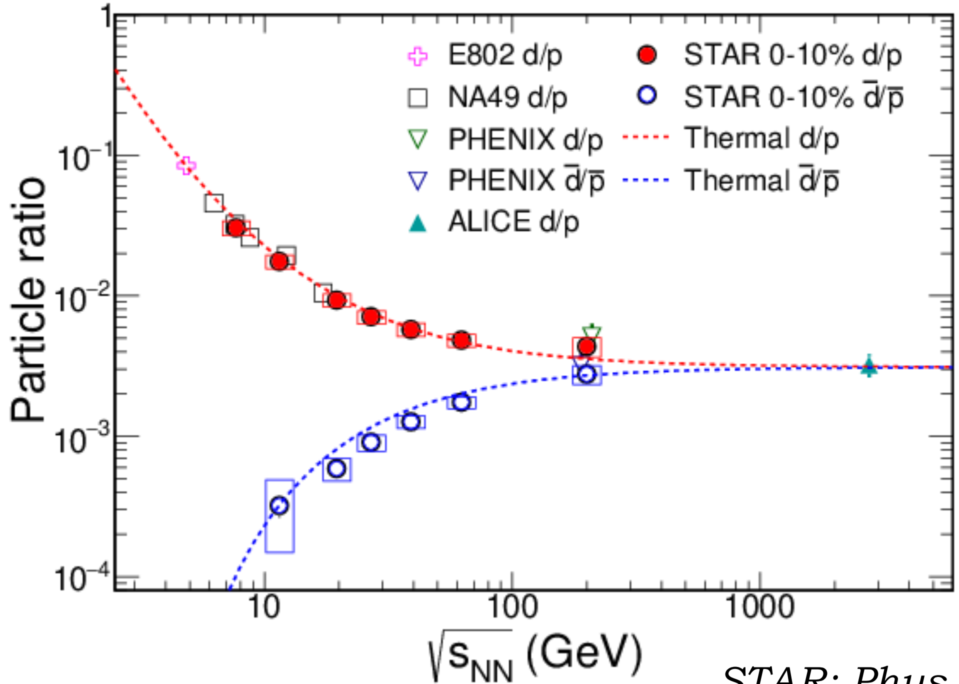

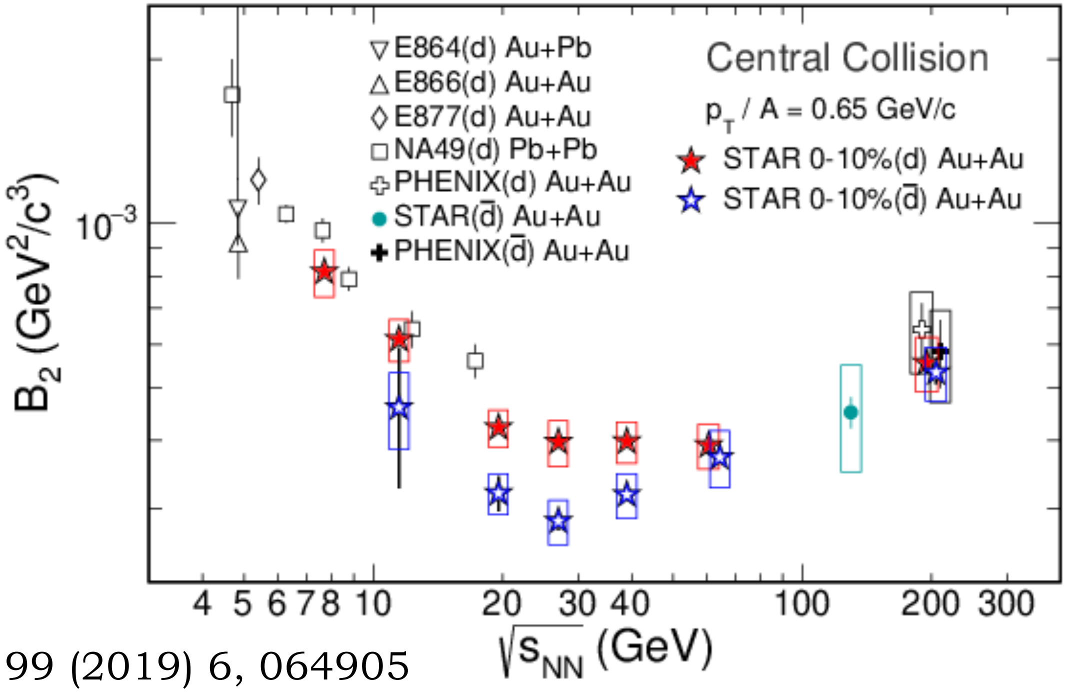

STAR: Phys.Rev.C 99 (2019) 6, 064905

1. Freeze-out properties similar to hadrons.
2. B_2 values reach a minimum at about $\sqrt{s_{NN}}$ =20–40 GeV. Change in EOS ?
3. B_2 (antideuterons) < B_2 (deuterons) below 62.4 GeV. Size of the emitting source of antibaryons is larger than that of baryons ?

Freeze-out (geometry)

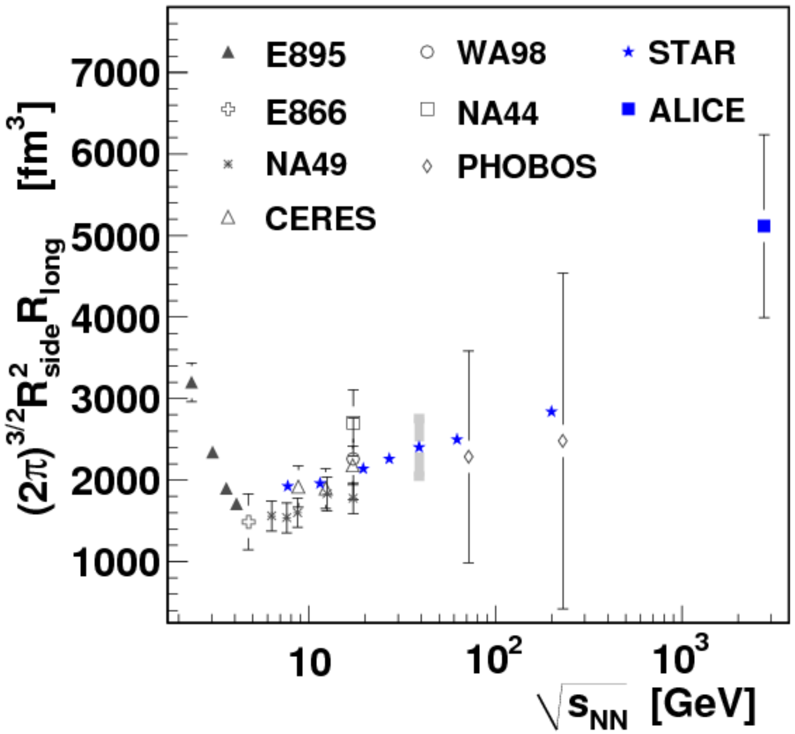

Non-monotonic variation of homogeneity region volume.

STAR: Phys.Rev.C 92 (2015) 1, 014904

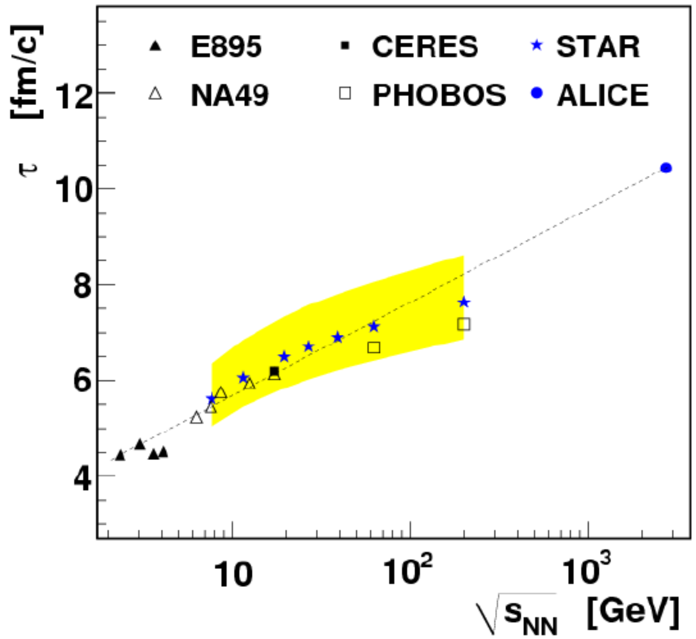

Lifetime of the system taking KFO temperature 120 MeV.

Freeze-out shape remains an out-of-plane extended ellipse ($\varepsilon_F>0$).

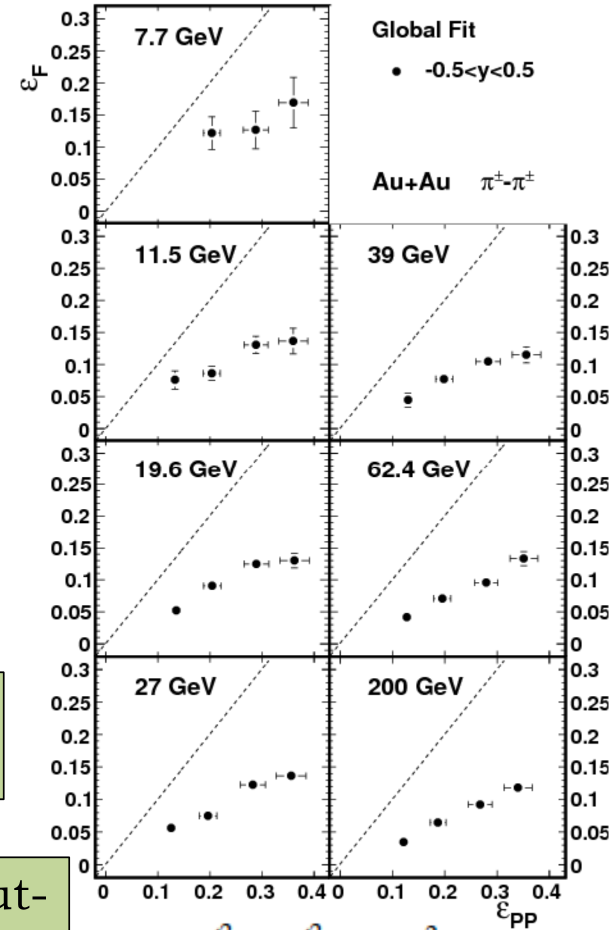

$$\varepsilon_F = \frac{\sigma_y'^2 - \sigma_x'^2}{\sigma_y'^2 + \sigma_x'^2} \approx 2\frac{R_{s,2}^2}{R_{s,0}^2}$$

Chemical freeze-out (conclusions)

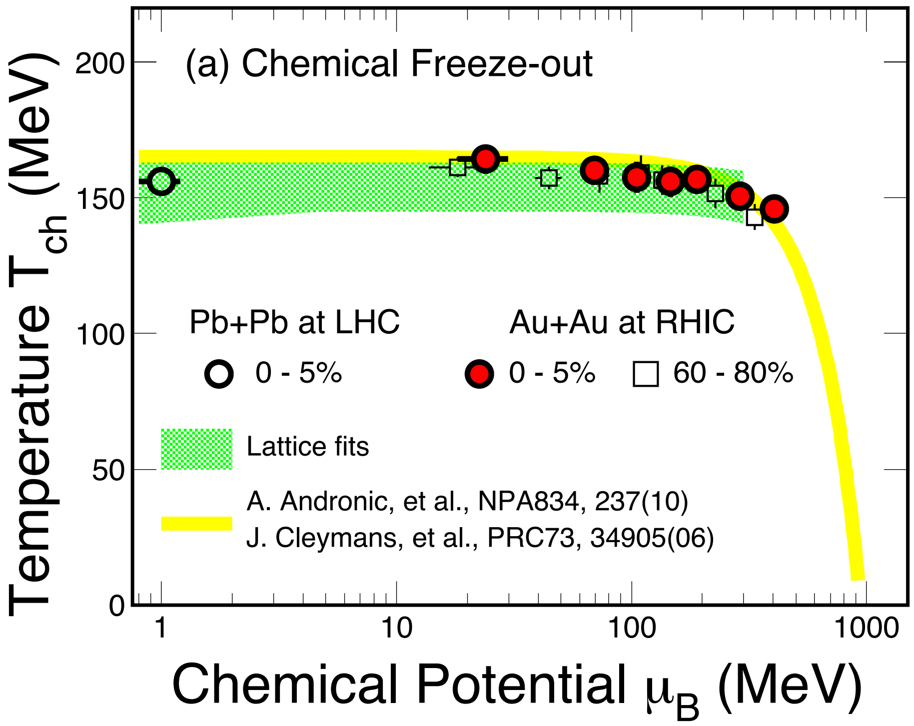

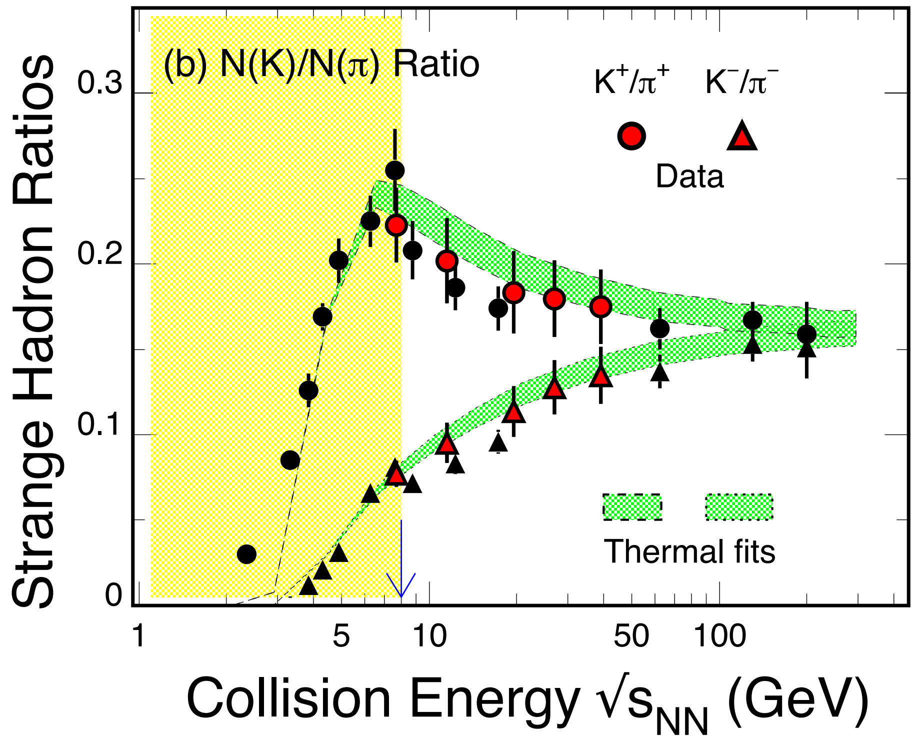

Chemical freeze-out: (GCE)
Close to LCD transition line
T weak and $\boldsymbol{\mu_B}$ stronger dependence on centrality

- The **K^+/π** ratio peaks at $\sqrt{s_{NN}}$ ~ 8 GeV where model also predicted the peak of baryon density
- **HBDR**: ($\sqrt{s_{NN}}$ < 8 GeV, $\mu_B \geq 420$ MeV)

- ALICE: B.Abelev et al., PRL **109**, 252301(12); PR **C88**, 044910(13).
- STAR: J. Adams, et al., **NPA757**, 102(05); PR **C96**, 044904(17); **PRC96**, 044904(17).
- J. Randrup and J. Cleymans, Phys. Rev. **C74**, 047901(06)

In discussion with N. Xu

Collectivity related measurements

Radial flow.
Directed flow.
Elliptic flow.

Equation of state.
Partonic collectivity.

Nuclei collectivity.

Based on STAR publications

Phys.Rev.C 96 (2017) 4, 044904
Phys.Rev.Lett. 112 (2014) 16, 162301
Phys.Rev.Lett. 120 (2018) 6, 062301
Phys.Rev.Lett. 110 (2013) 14, 142301
Phys.Rev.C 94 (2016) 3, 034908
Phys.Rev.C 88 (2013) 014902
Phys.Rev.Lett. 116 (2016) 11, 112302
Phys.Rev.C 86 (2012) 054908
Phys.Rev.C 93 (2016) 1, 014907

Collectivity (radial flow)

Elastic collisions ceases

Blast-Wave Model

$$\frac{dN}{p_T dp_T} \propto \int_0^R r dr m_T I_0\left(\frac{p_T \sinh \rho(r)}{T_{kin}}\right) \times K_1\left(\frac{m_T \cosh \rho(r)}{T_{kin}}\right)$$

Parameters: Temperature (T_{kin}) and transverse radial velocity (β) obtained by fitting the momentum distribution of particles.

Features:
- Approximates hydrodynamic models
- Assumes particles are locally thermal and moving with a common velocity.

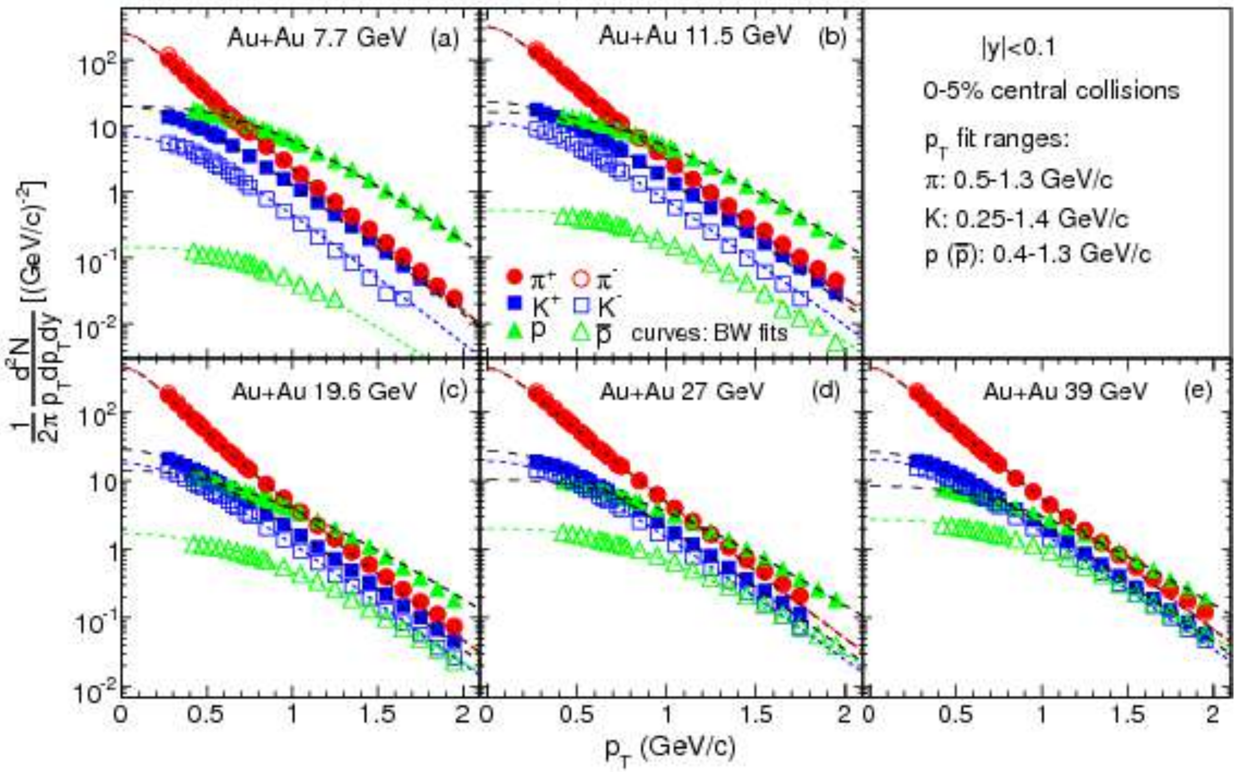

STAR: Phys.Rev.C 96 (2017) 4, 044904

E. Schnedermann, J. Sollfrank, and U. W. Heinz, Phys. Rev. C 48, 2462 (1993).

Collectivity (radial flow)

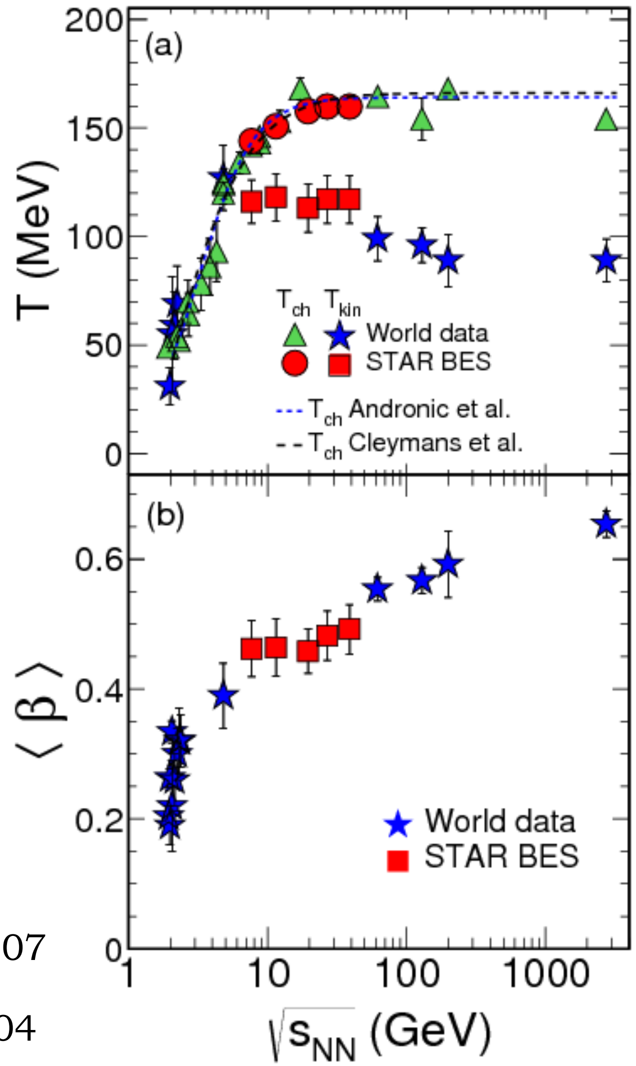

Radial flow stay constant at lower BES energies.

STAR: Phys.Rev.C 93 (2016) 1, 014907

STAR: Phys.Rev.C 96 (2017) 4, 044904

Collectivity (azimuthal anisotropy)

Initial spatial anisotropy

Pressure gradient

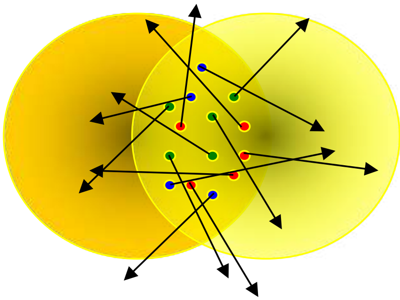

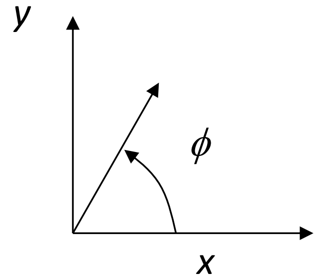

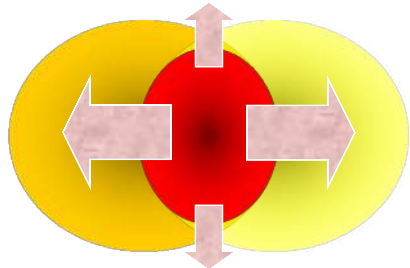

INPUT Spatial Anisotropy

Interaction among produced particles

OUTPUT Momentum Anisotropy

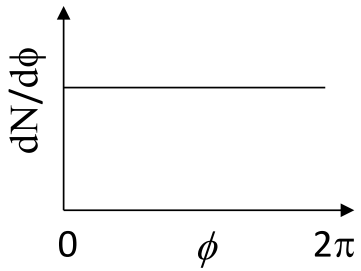

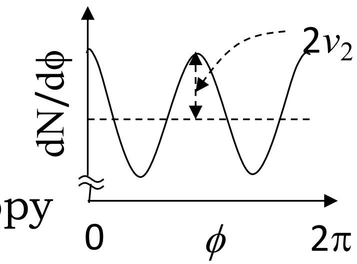

$$\varepsilon_x = \left\langle \frac{y^2 - x^2}{y^2 + x^2} \right\rangle$$

$\lambda = (\sigma\rho)^{-1}$

$c_s^2 = dP/d\varepsilon$

$$v_2 = \langle \cos 2\varphi \rangle = \left\langle \frac{p_x^2 - p_y^2}{p_x^2 + p_y^2} \right\rangle$$

Free streaming
v_2 (elliptic flow) =0

$v_1 = \langle \cos\varphi \rangle$ Directed flow

Collectivity (slope of directed flow vs. rapidity)

STAR: Phys.Rev.Lett. 112 (2014) 16, 162301

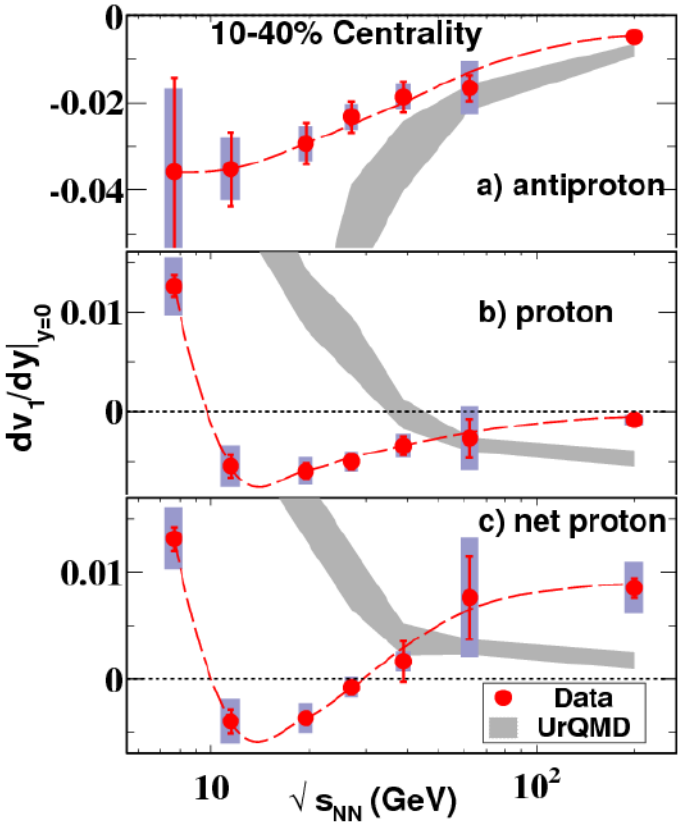

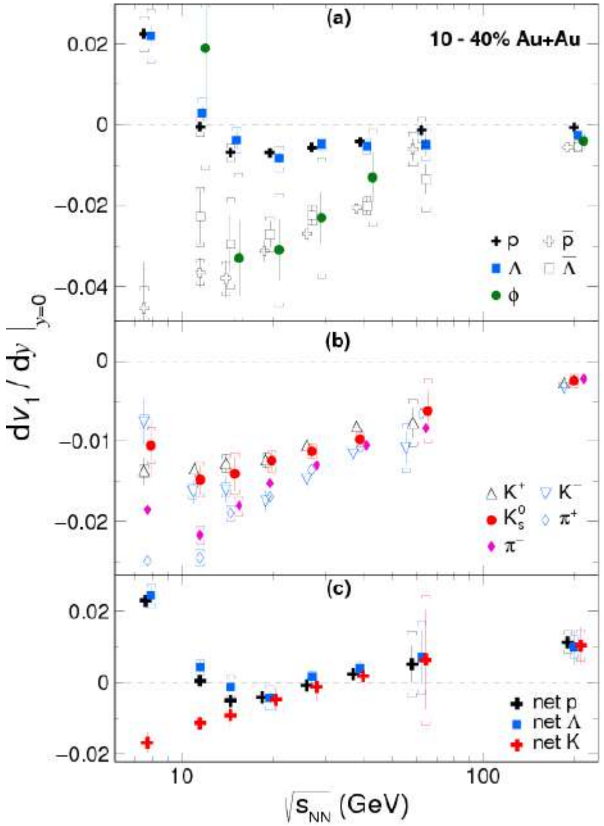

STAR: Phys.Rev.Lett. 120 (2018) 6, 062301

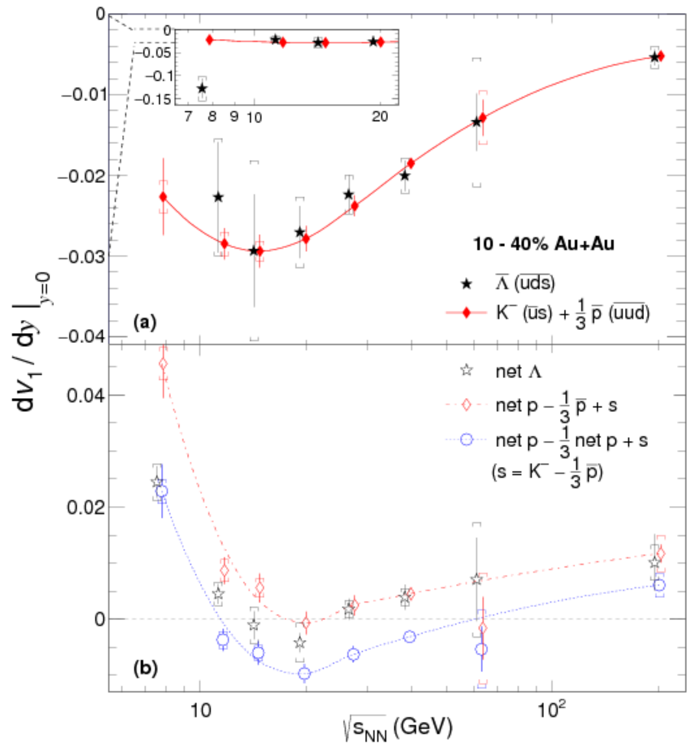

1) Non-monotonic variation of directed flow slope with collision energy for net-baryons.
2) Net-kaons show monotonic variations of directed flow slope with collision energy.
3) Coalescence sum rules are tested.

Collectivity (elliptic flow)

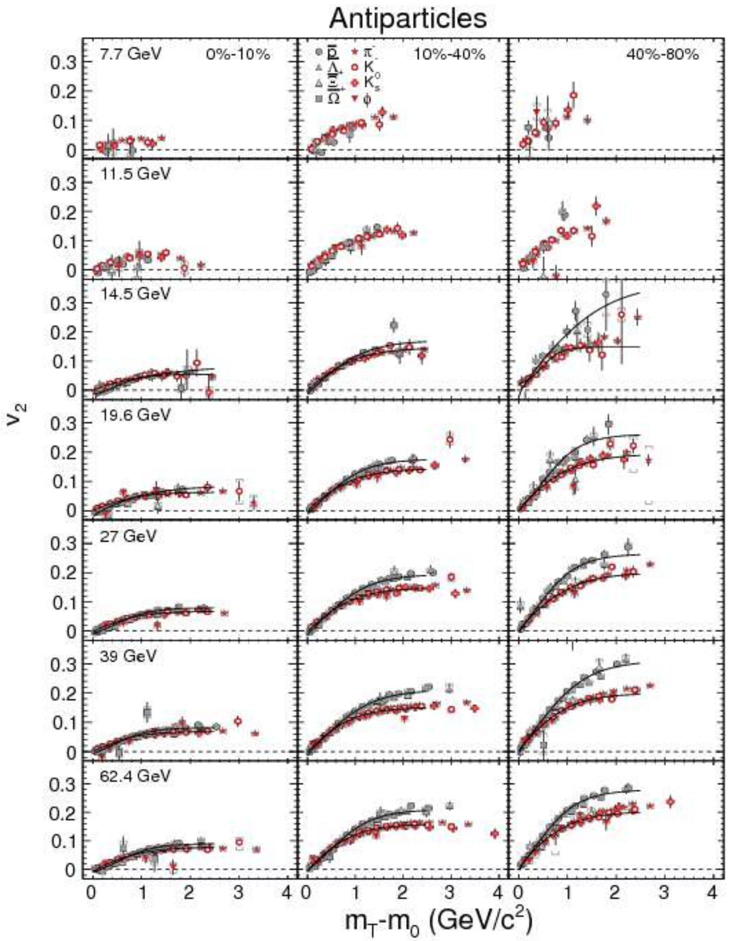

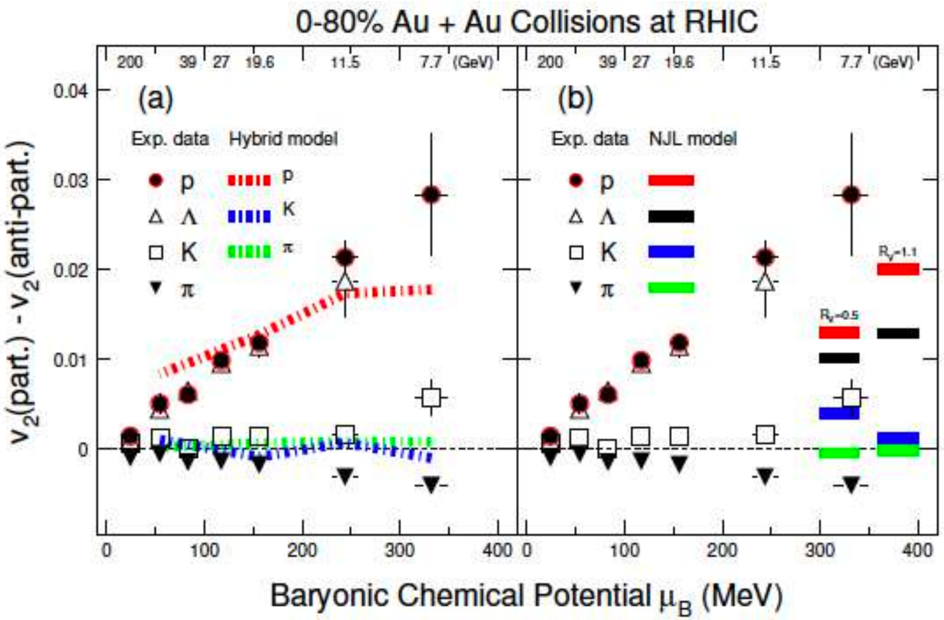

STAR: Phys.Rev.Lett. 110 (2013) 14, 142301
Phys.Rev.C 88 (2013) 014902

Breakdown of NCQ scaling of elliptic flow as seen at top RHIC energy of 200 GeV

1. Baryon-meson difference at intermediate p_T reduces as collision energy decreases
2. Difference between particle and anti-particle v_2 increases as μ_B increases. Mean field calculations suggest links to baryon density.

Collectivity (elliptic flow nuclei)

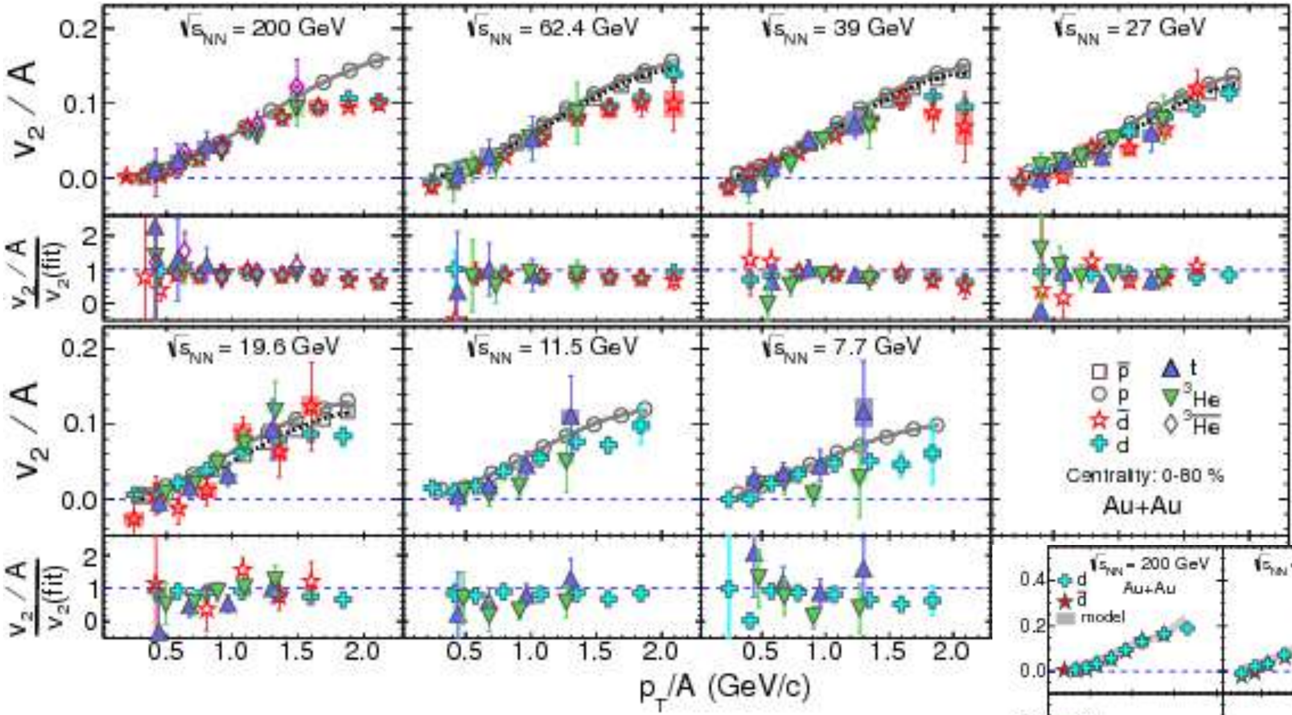

STAR: Phys.Rev.C 94 (2016) 3, 034908

Nuclei v_2 flows mass number scaling, indicating they are formed via coalescence.

Nuclei v_2 described well by a coalescence model incorporated in AMPT.

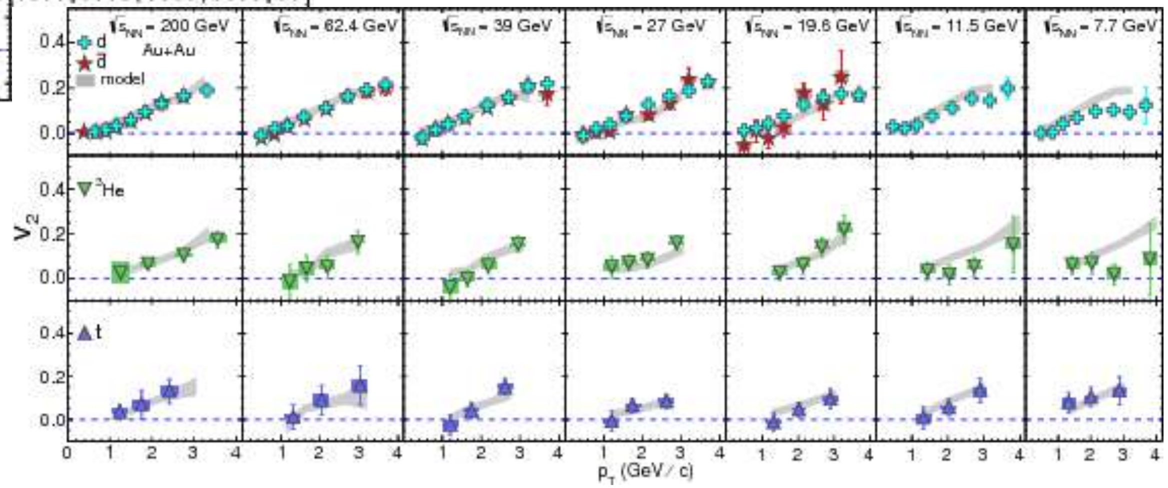

Collectivity (conclusions)

ϕ flow ≡ partonic collectivity

1. BES-I: Wealth of data to test coalescence mechanisms and obtain medium properties.
2. At lower collision energies, **dominance of hadronic interactions over partonic interactions**.
3. **Non-monotonic variations** in net-baryon directed flow slope and v_3 fluctuations with collision energy observed.
4. **Differences** between collectivity of **particles and anti-particles** observed. Indicating sensitivity to medium properties.
5. In **BES-II**: **Precision** measurements of **ϕ-meson flow** will shed further light on partonic collectivity.
6. Theoretical attempts to understand the EOS and **extracting η/s for high baryon density matter** have started.

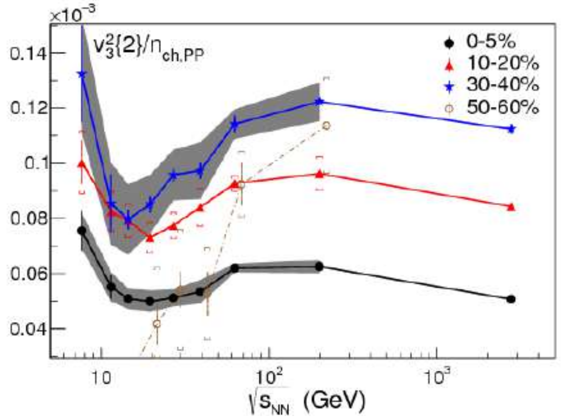

STAR: Phys.Rev.Lett. 116 (2016) 11, 112302

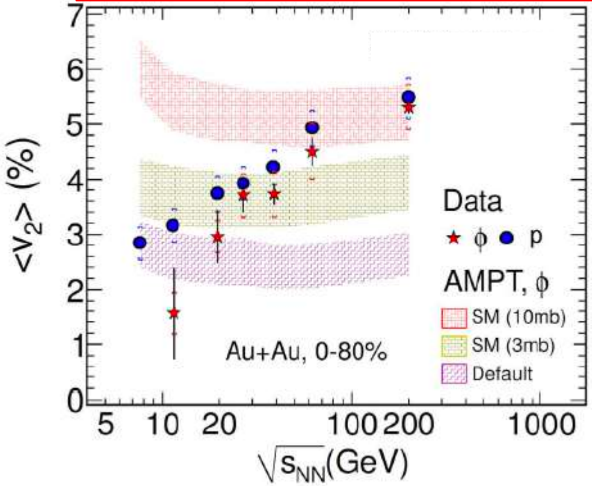

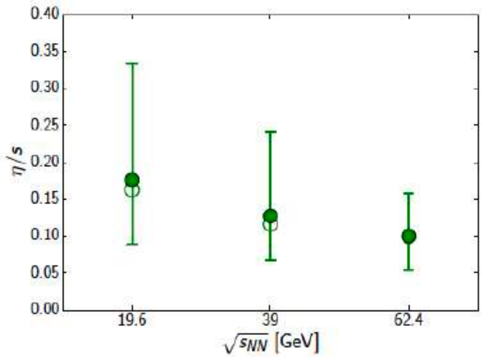

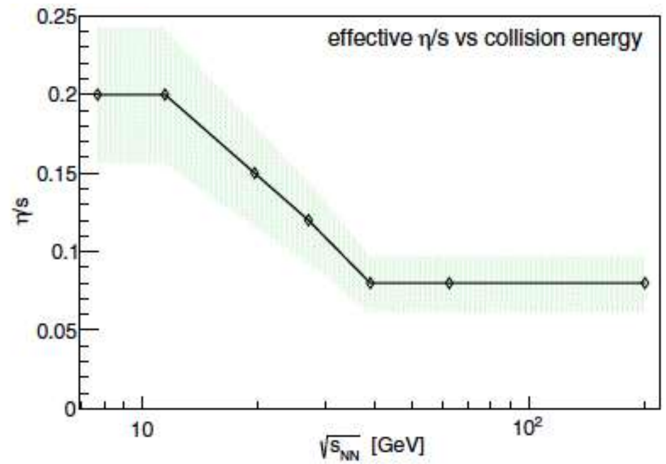

Phys. Rev. C 91, 064901 (2015)
Phys.Rev.C 97 (2018) 4, 044905

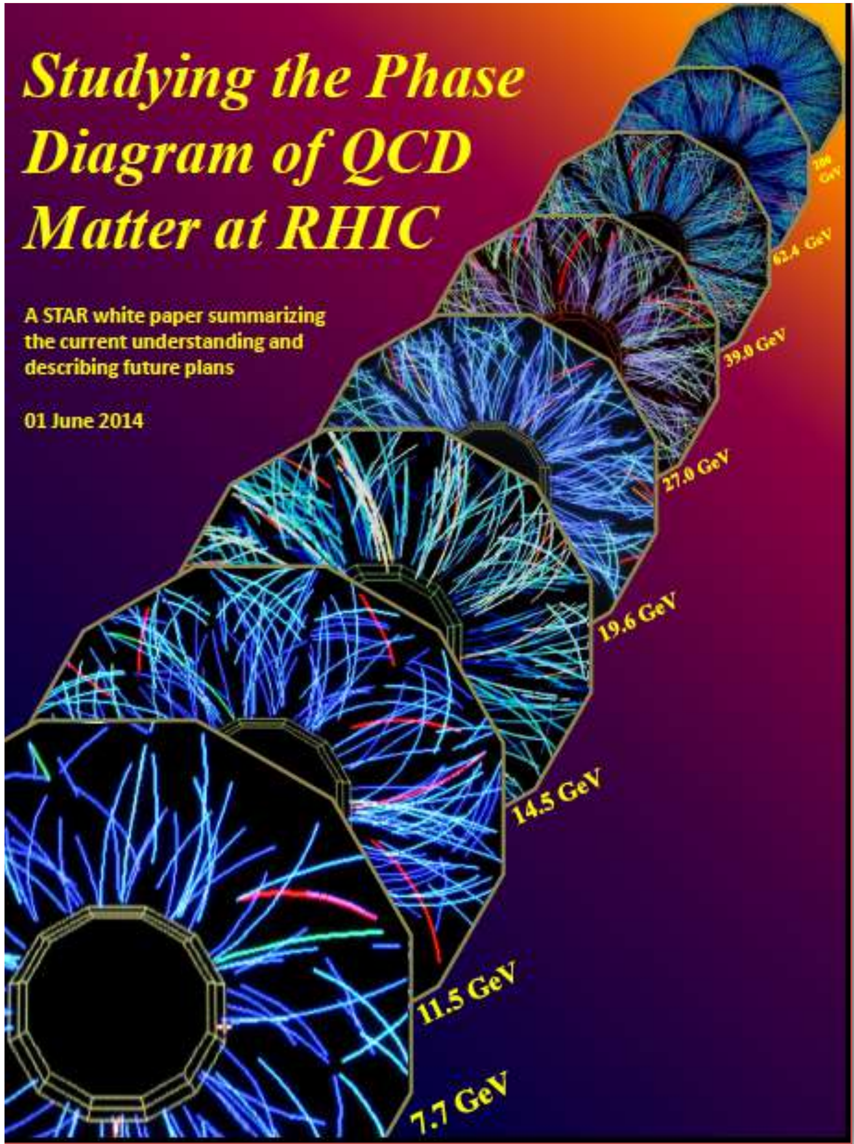

Criticality related measurements

Based on STAR publications
arXiv: 2001.02852
Phys.Rev.Lett. 112 (2014) 032302
Phys.Rev.Lett. 113 (2014) 092301
Phys.Lett.B 785 (2018) 551-560
Phys.Rev.C 100 (2019) 1, 014902
Phys.Rev.C 99 (2019) 4, 044918
Phys.Rev.C 101 (2020) 1, 014916
Phys.Rev.C 94 (2016) 2, 024909
Phys.Rev.C 92 (2015) 2, 021901

Criticality

Developed at INT'2008

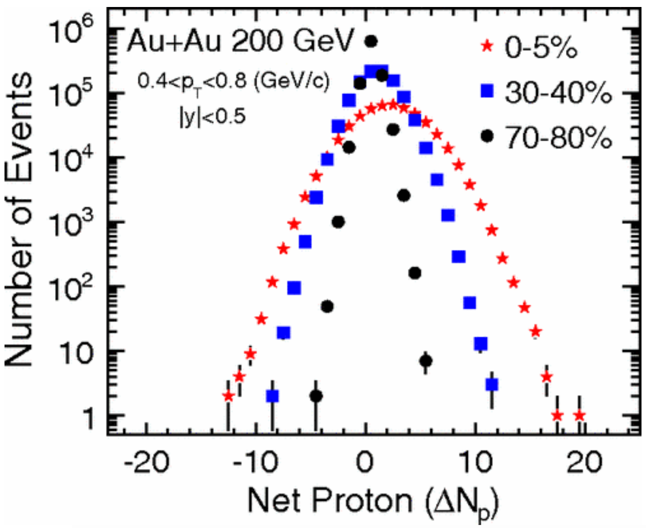

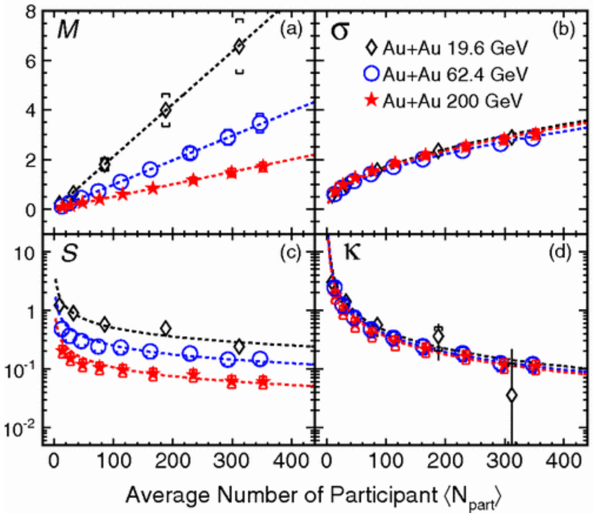

First measurements – 2009-2010

1) High moments of conserved quantum numbers: ***Q, S, B***, in high-energy nuclear collisions

2) Sensitive to critical point (ξ correlation length):

$$\langle(\delta N)^2\rangle \approx \xi^2, \ \langle(\delta N)^3\rangle \approx \xi^{4.5}, \ \langle(\delta N)^4\rangle \approx \xi^7$$

3) Direct comparison with calculations at any order:

$$S\sigma \approx \frac{\chi_B^3}{\chi_B^2}, \qquad \kappa\sigma^2 \approx \frac{\chi_B^4}{\chi_B^2}$$

4) Extract susceptibilities and freeze-out temperature. An independent/important test of thermal equilibrium in heavy ion collisions.

References:- STAR: *PRL* **105**, 22303(10); *ibid*, **112**, 032302(14); S. Ejiri, F. Karsch, K. Redlich, *PLB***633**, 275(06); M. Stephanov: *PRL***102**, 032301(09) ; F. Karsch *et al.*, *PLB***695**, 136(11); R.V. Gavai and S. Gupta, *PLB***696**, 459(11); A. Bazavov *et al.*, PRL**109**, 192302(12); V. Skokov *et al.*, PRC**88**, 034901(13); S. Borsanyi *et al.*, PRL**111**, 062005(13); PBM, A. Rustamov, J. Stachel, NPA**960**, 114(17); A. Bzdak, *et al.*, arXiv: 1906.00936, Physics Report, **853C**, 1(2020)

Criticality (Model)

See Talk my M. Stephanov on 11th August 2020

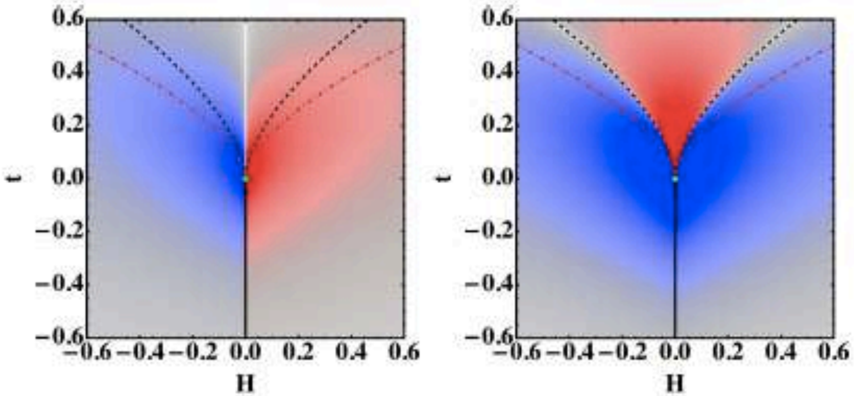

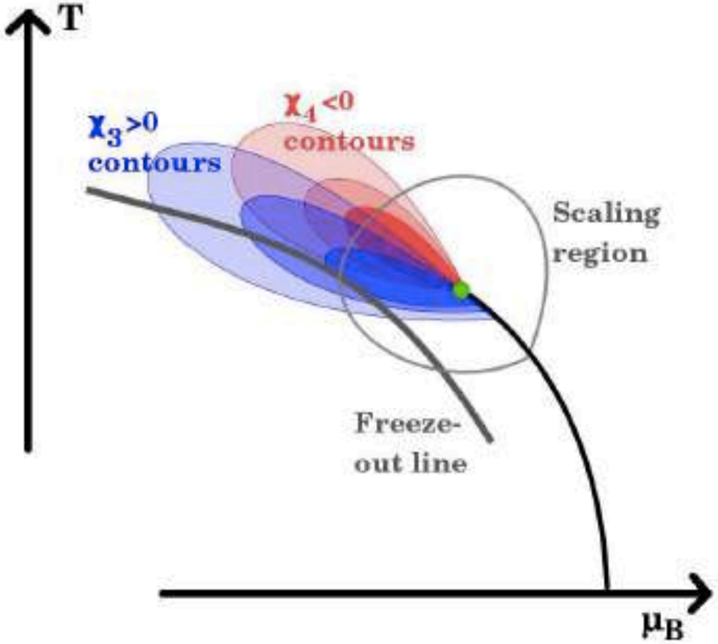

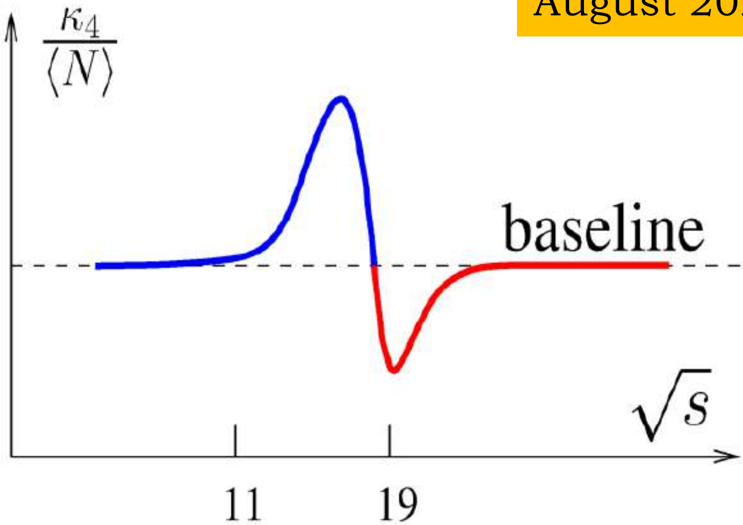

- Characteristic "Oscillating pattern" is expected for the QCD critical point but *the exact shape depends on the location of freeze-out with respect to the location of CP*
- Critical Region (CR)

  - M. Stephanov, ***PRL107***, 052301(2011)
  - V. Skokov, Quark Matter 2012
  - J.W. Chen, J. Deng, H. Kohyyama, Phys. Rev. **D93** (2016) 034037

Criticality (net-charge and net-kaon)

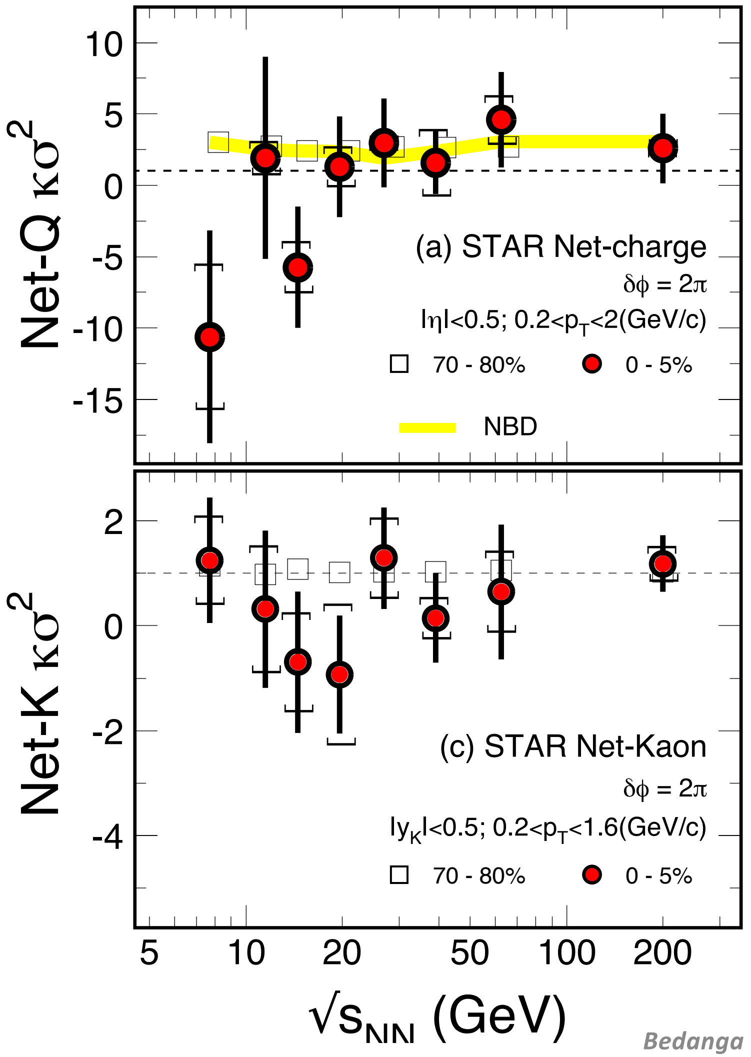

1) The results of net-Q and net-Kaon show flat energy dependence
2) The statistical uncertainty

$$\sim \frac{\sigma^m}{\sqrt{N}\,\varepsilon^k}$$

STAR
Phys.Rev.Lett. 113 (2014) 092301
Phys.Lett.B 785 (2018) 551-560

Criticality (Data)

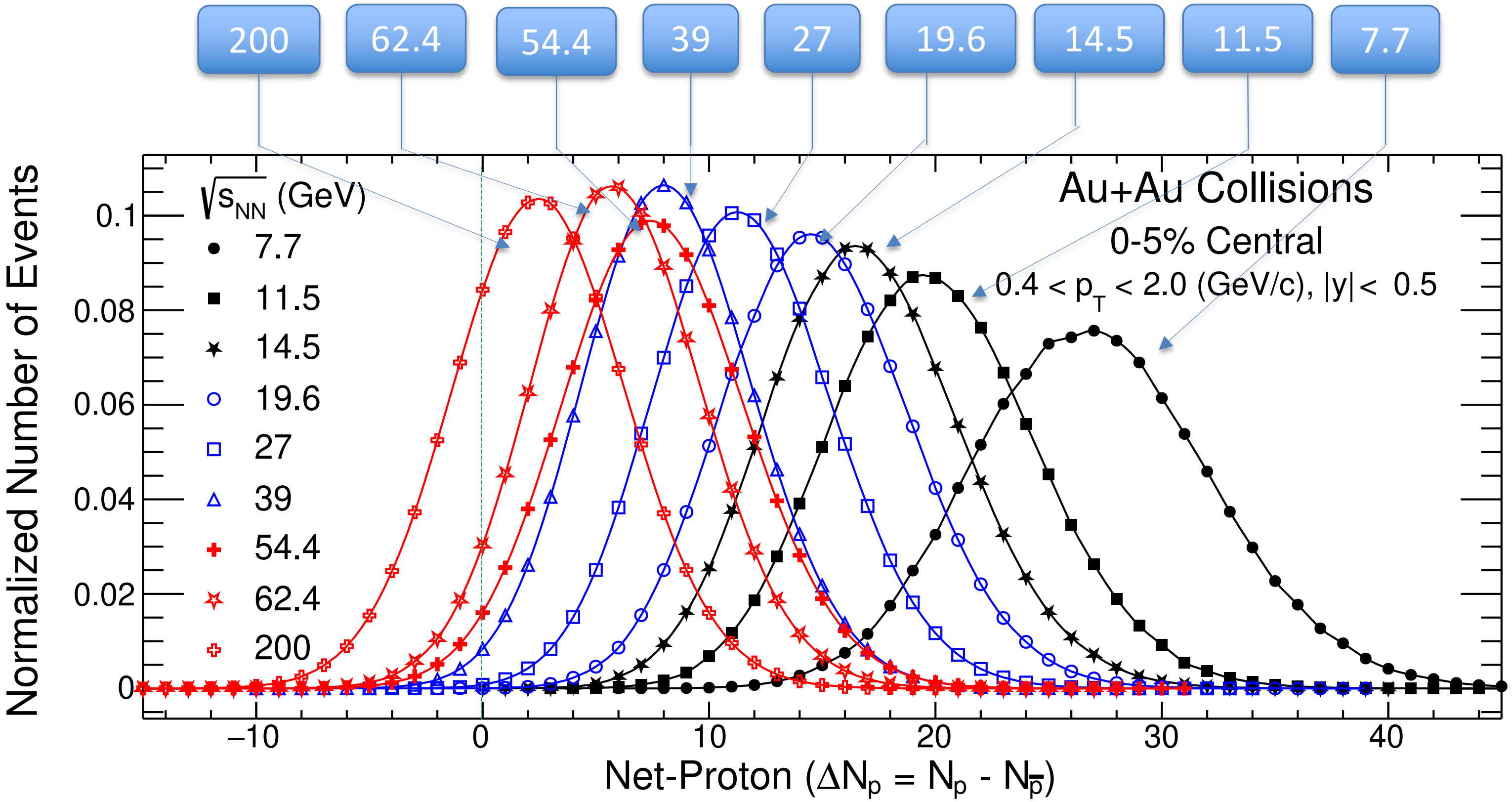

1) Net-proton distributions, top 5% central collisions, efficiency uncorrected.
2) Value of mean and the width increase as energy decreases, effect of baryon stopping.

STAR: arXiv: 2001.02852

Criticality (non-monotonic)

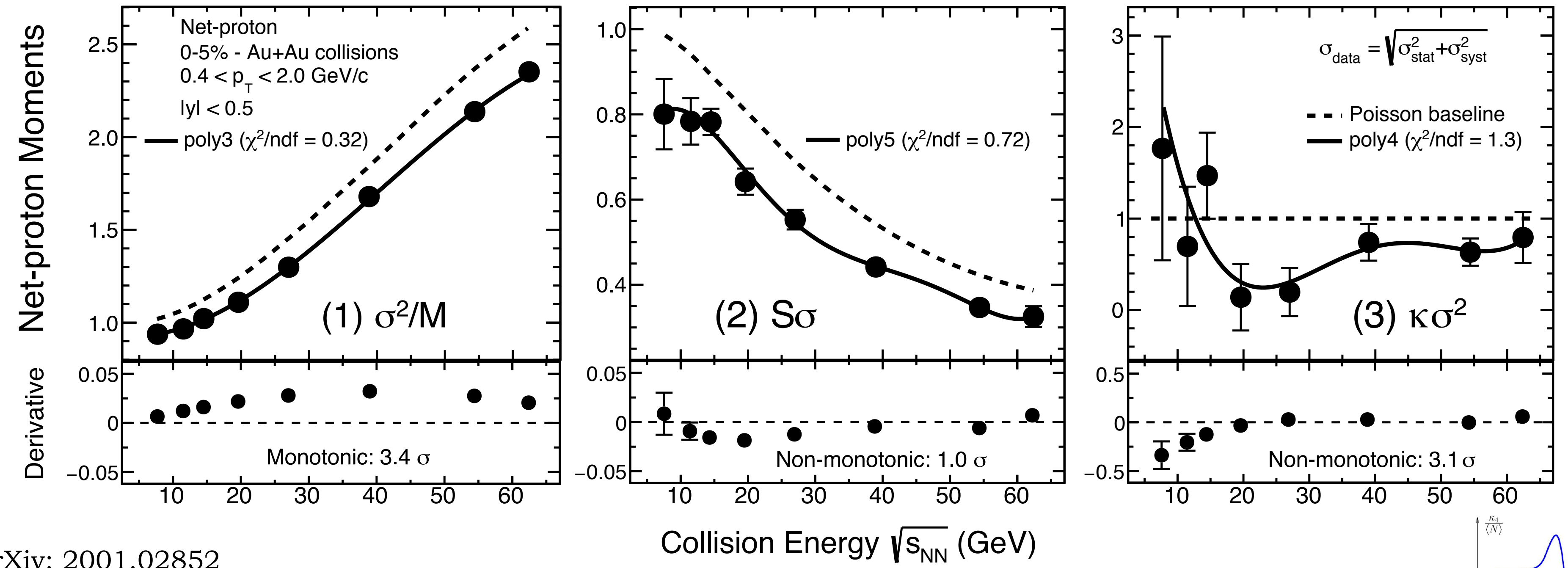

STAR: arXiv: 2001.02852

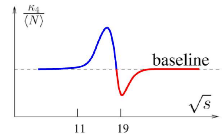

Data	Monotonic	~ Non-Monotonic	Non-Monotonic
Theory	$\langle(\delta N)^2\rangle \approx \xi^2$	$\langle(\delta N)^3\rangle \approx \xi^{4.5}$	$\langle(\delta N)^4\rangle \approx \xi^7$

M. Stephanov: *PRL* **102**, 032301(09)

Higher moments/cumulants are sensitive observables.

Criticality (net-proton)

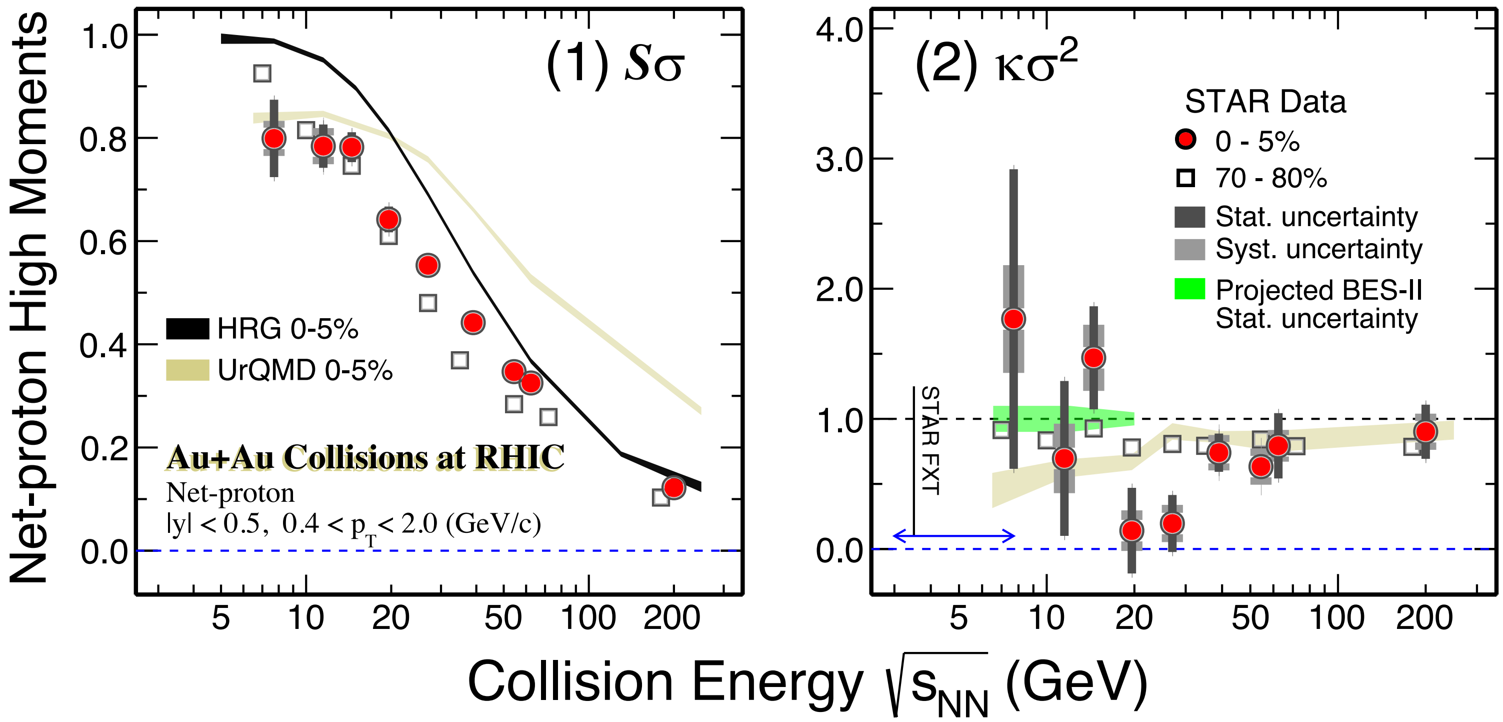

1) Ratios of the net-proton cumulants, top 5% central and 70-80% peripheral collisions.
2) Net-proton: **non-monotonic energy dependence** in the most central Au+Au collisions.

STAR: arXiv: 2001.02852

Criticality (comparison to models)

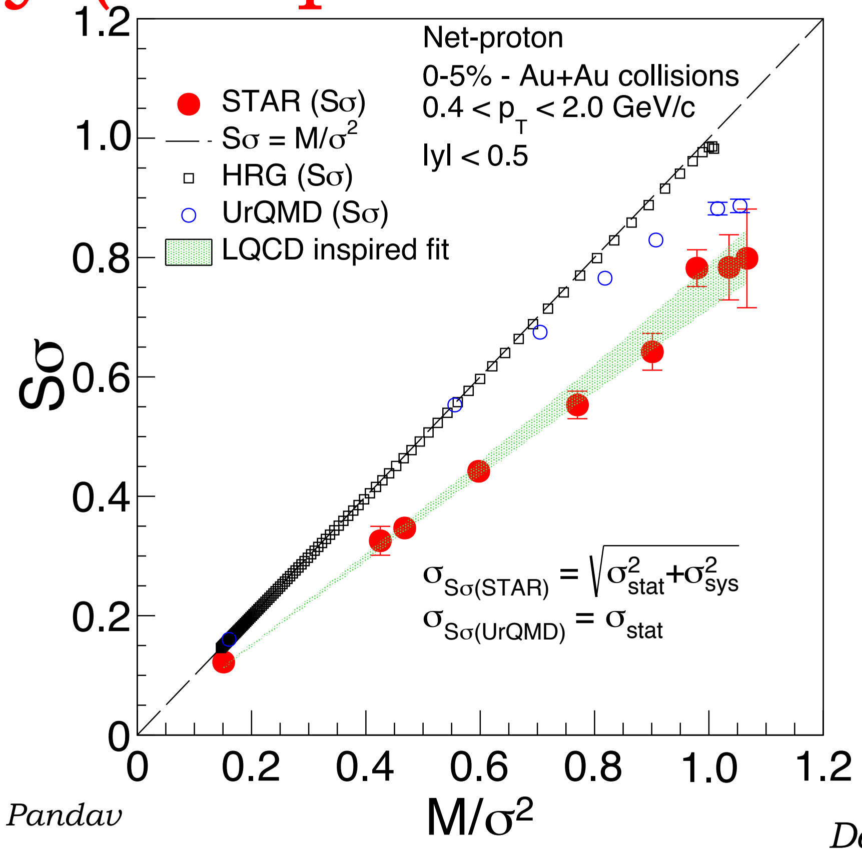

In discussion with F. Karsch, N. Xu and A. Pandav

Data STAR: arXiv: 2001.02852

- ✓ Higher collision energy data and LQCD (inspired) features similar.
- ✓ Deviations from HRG and UrQMD
  → Strongly interacting QCD matter

Criticality (other measurements)

Phys.Rev.C 94 (2016) 2, 024909

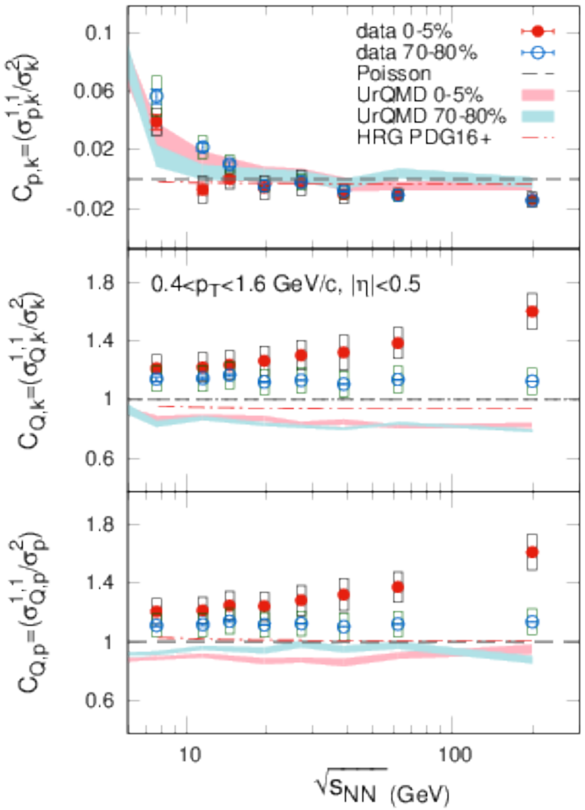

Phys.Rev.C 101 (2020) 1, 014916

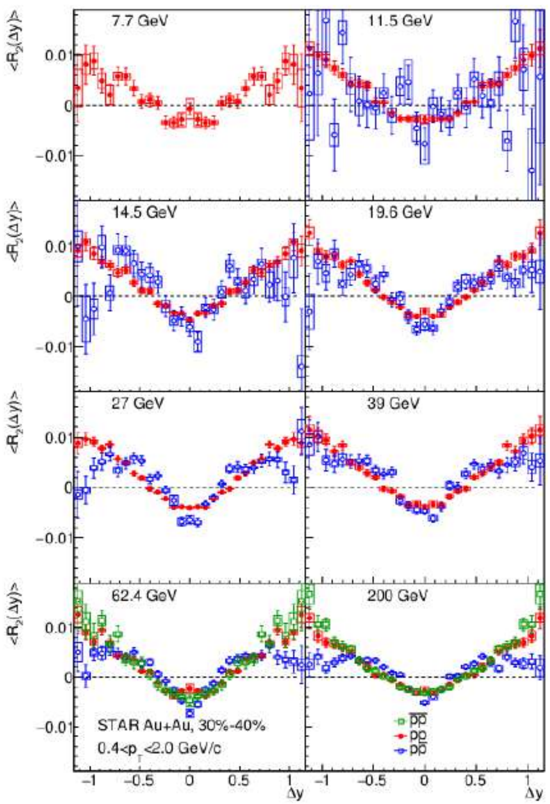

Phys.Rev.C 99 (2019) 4, 044918

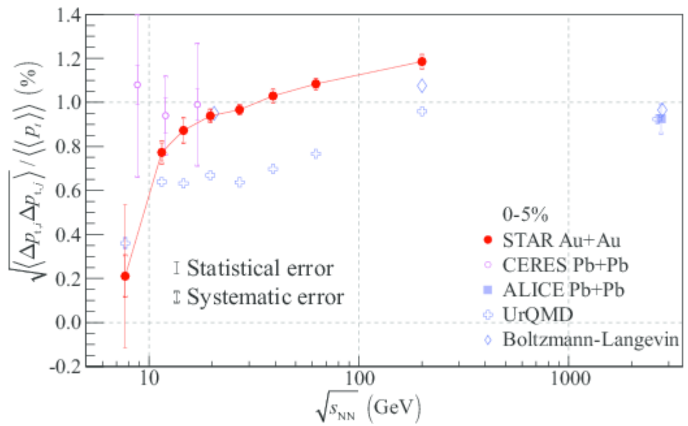

Phys.Rev.C 92 (2015) 2, 021901

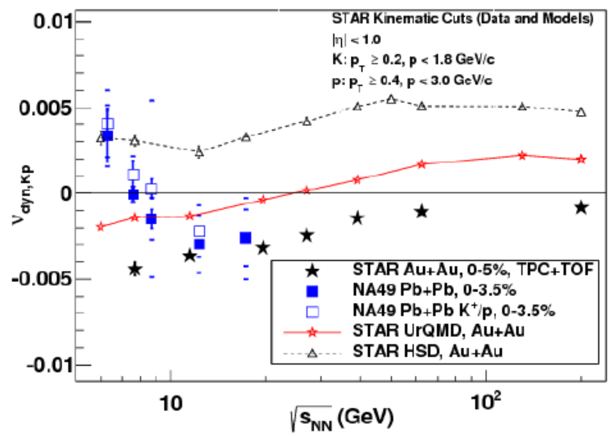

(1) Charge-baryon-strangeness correlations (2) Rapidity correlations (anti-correlations for protons) (3) p_T correlations

Criticality (conclusions)

1) **Non-monotonic variation of** $\kappa\sigma^2$ with collision energy observed with **3 sigma significance**.

2) **BES-II** is underway. The focus is in the region of **7.7 – 19.6 GeV** in collider mode to improve statistical precision of the measurements.

Chirality related measurements

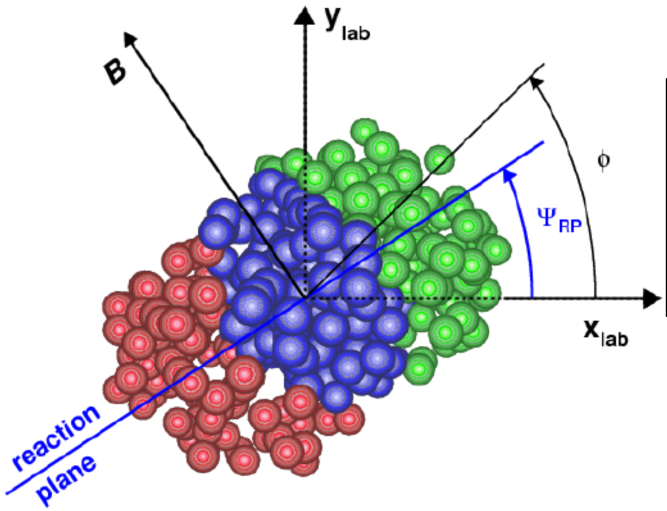

Based on STAR publications
Phys.Rev.Lett. 113 (2014) 052302
Phys.Rev.Lett. 114 (2015) 25, 252302
Nature 548 (2017) 62-65

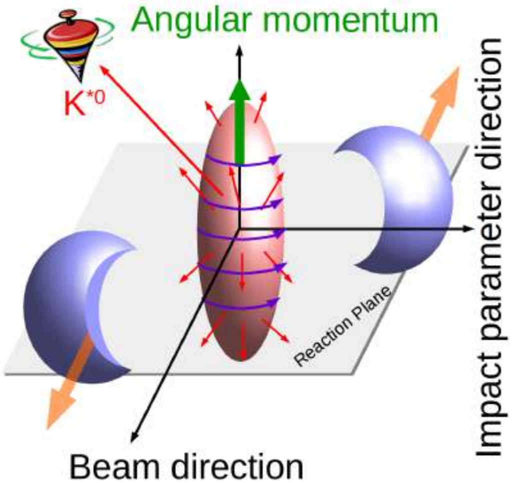

Chirality effects

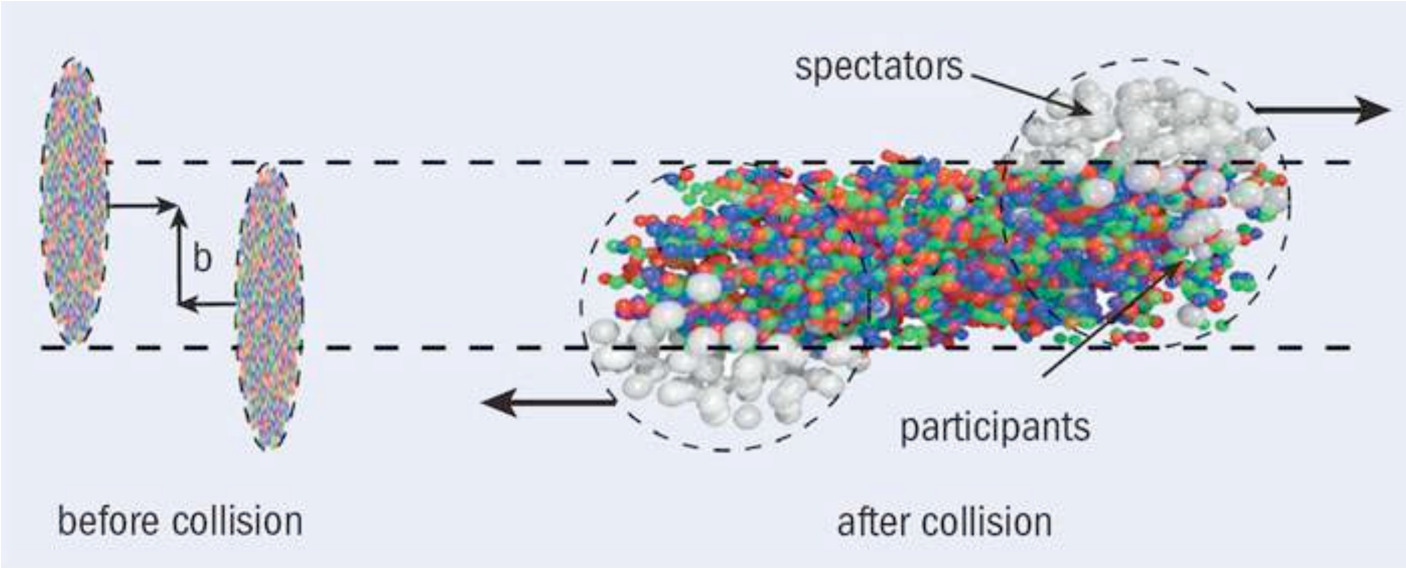

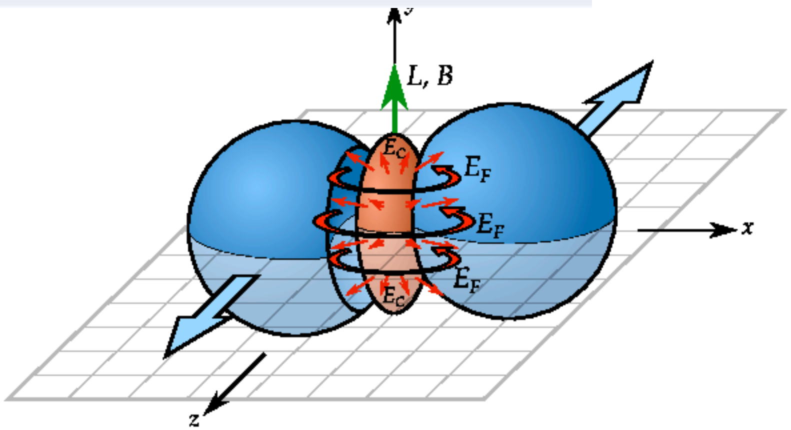

Reaction plane: Impact parameter and beam axis

L and B perpendicular to reaction plane

Chirality (magnetic field and angular momentum)

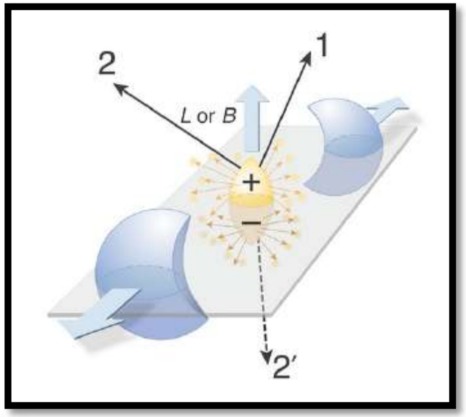

Impact parameter dependence

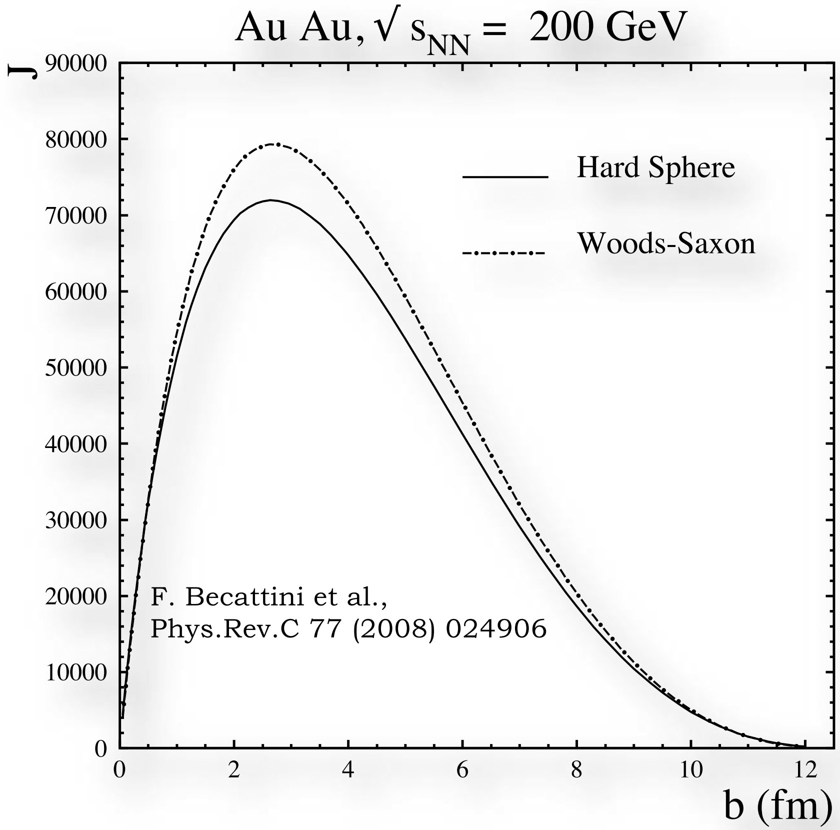

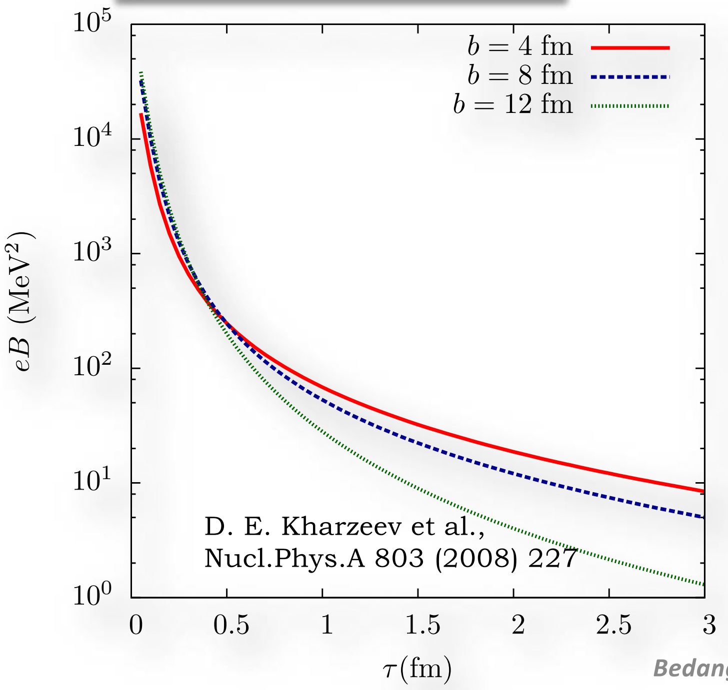

Time dependence

Large magnetic field

M^2_π ~ 2 x 10^4 MeV^2 ~ 3 x 10^{14} Tesla
~ 3 x 10^{18} Gauss

Large angular momentum
(Conserved Quantity)

Chirality (chiral magnetic effect)

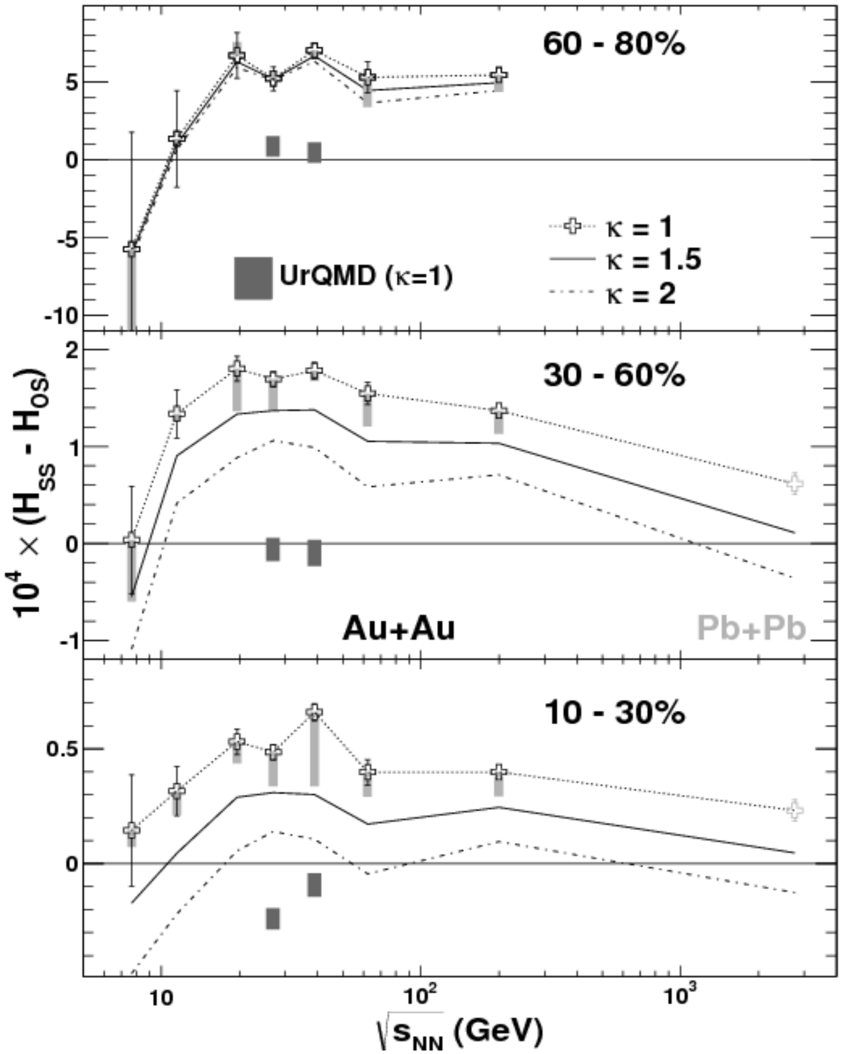

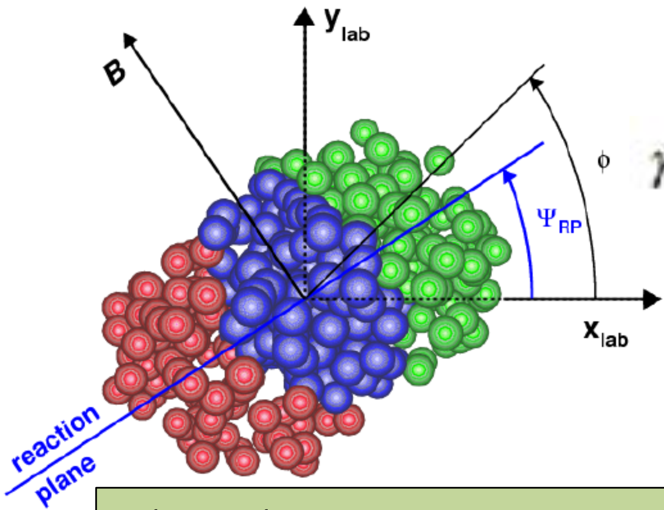

$$\gamma \equiv \langle \cos(\phi_1 + \phi_2 - 2\Psi_{RP}) \rangle$$

The charge separation along the magnetic field, shows a signal with a weak energy dependence down to19.6 GeV and then falls steeply at lower energies. This trend may be consistent with the hypothesis of local parity violation. Alternate hypothesis exits. Dedicated isobar run at RHIC.

STAR: Phys.Rev.Lett. 113 (2014) 052302

Chirality (chiral magnetic wave)

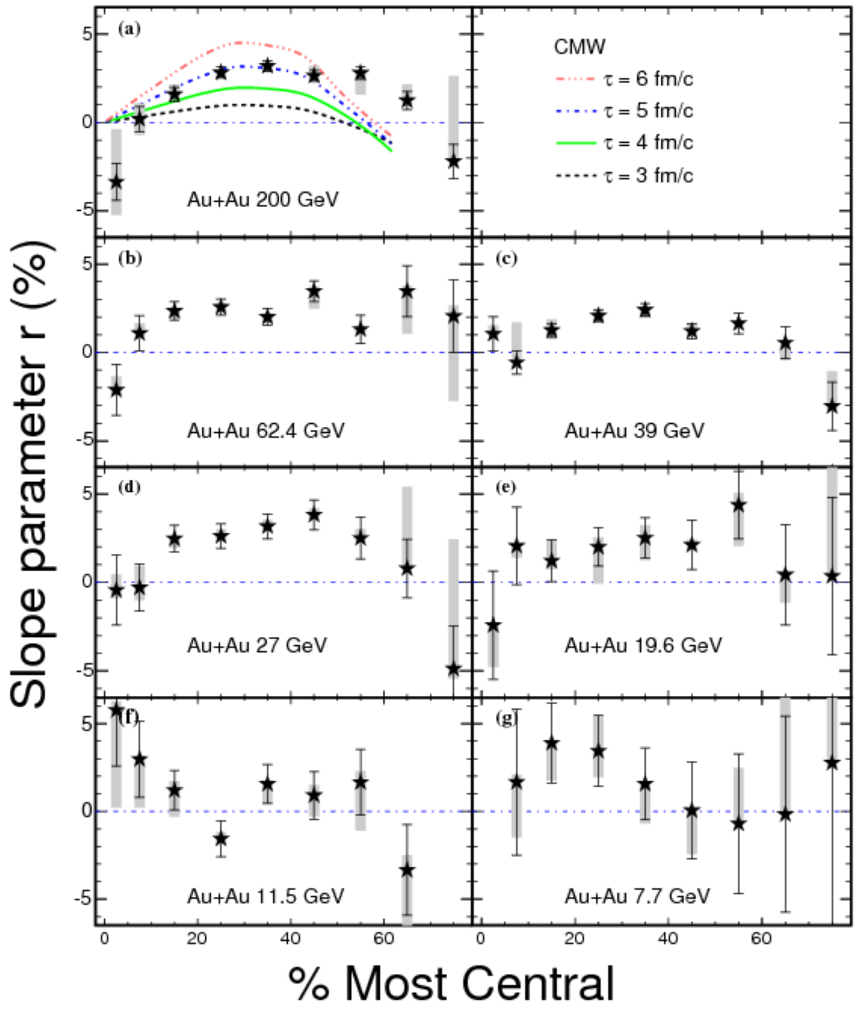

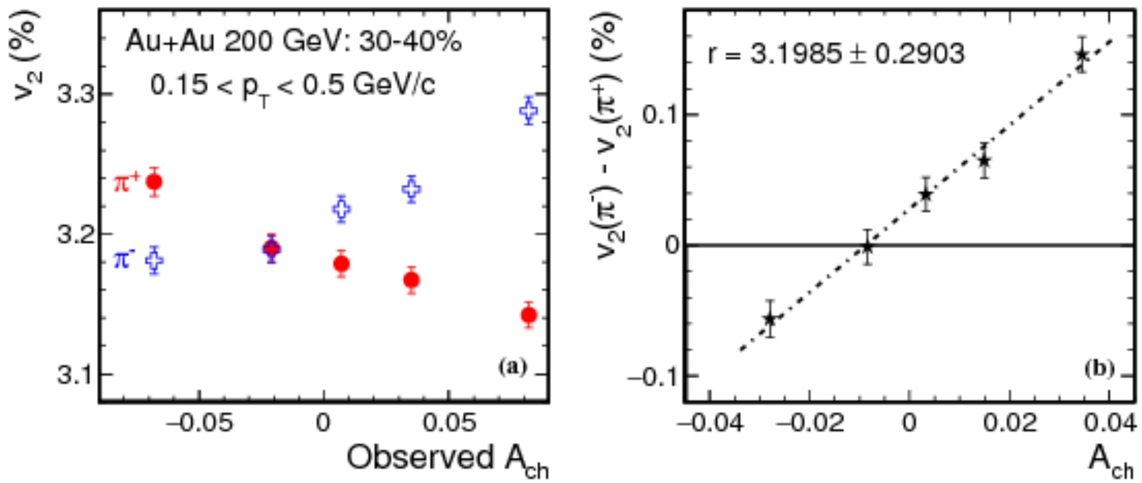

The v_2 difference between negatively and positively charged pions increases as a function of Ach [$(N^+ - N^-)/(N^+ + N^-)$], qualitatively reproducing the expectation from the CMW model.
The slope (r) shows no obvious trend of the beam energy dependence with the current statistics

STAR: Phys.Rev.Lett. 114 (2015) 25, 252302

Lambda polarization

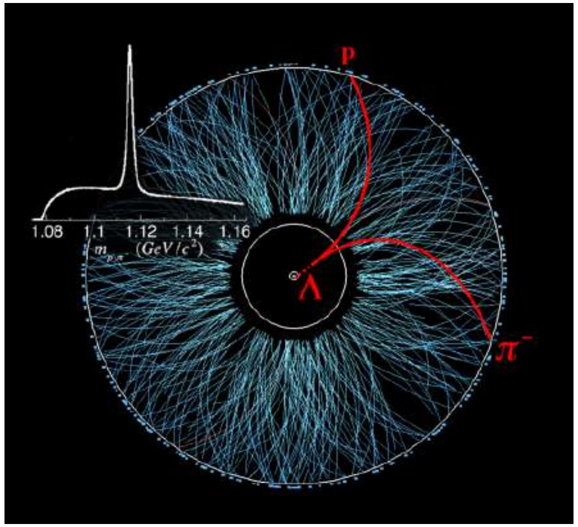

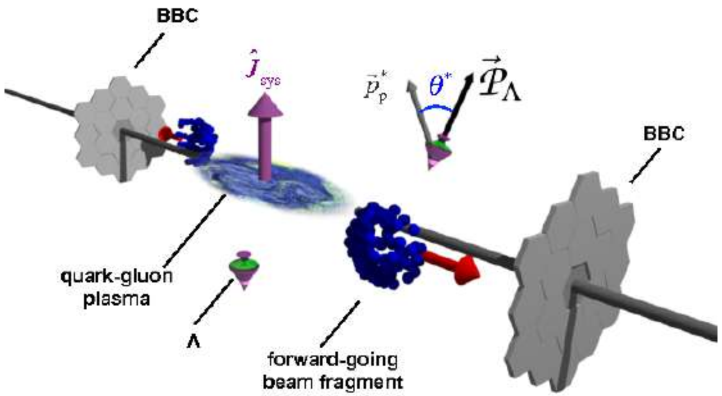

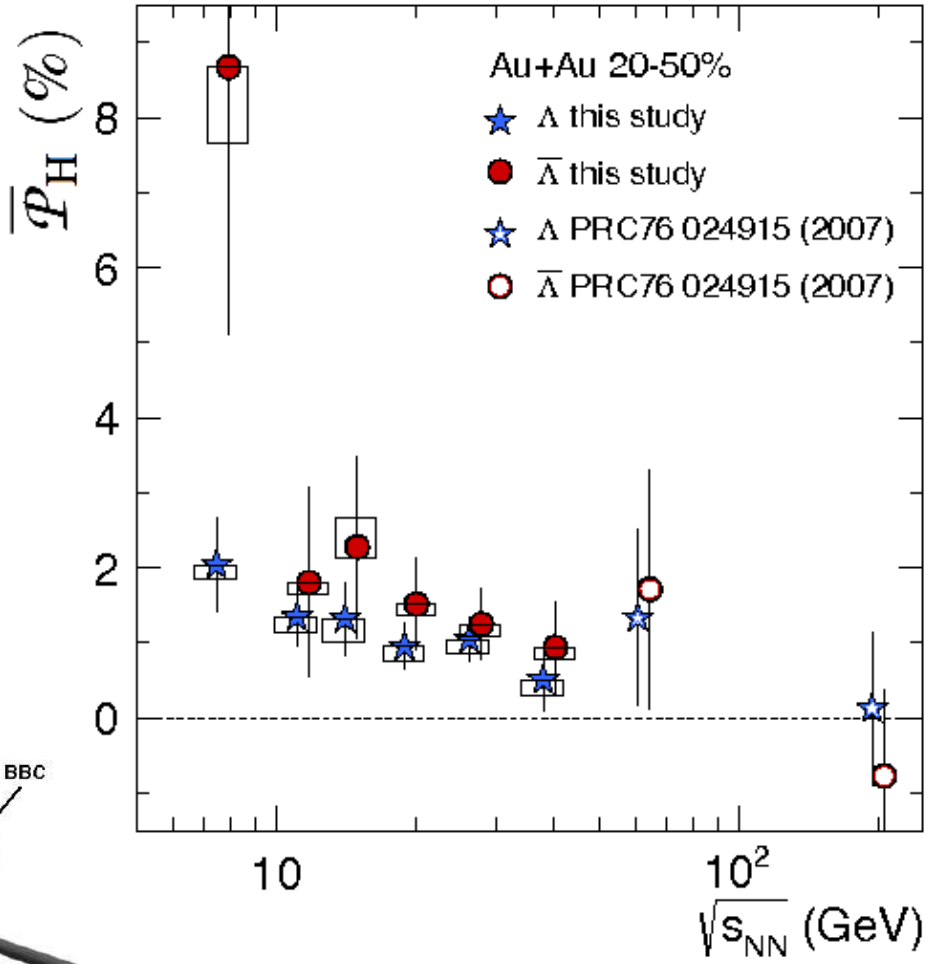

STAR: Nature 548 (2017) 62-65

$$\frac{dN}{d\cos\theta^*} = \frac{1}{2}\left(1+\alpha_H|\vec{\mathcal{P}}_H|\cos\theta^*\right)$$

$$\omega = k_B T\left(\overline{\mathcal{P}}_{\Lambda'} + \overline{\mathcal{P}}_{\overline{\Lambda}'}\right)/\hbar$$

$$\omega \approx (9 \pm 1) \times 10^{21}\ \mathrm{s}^{-1}$$

Vorticial fluid created at RHIC

Vector meson spin alignment

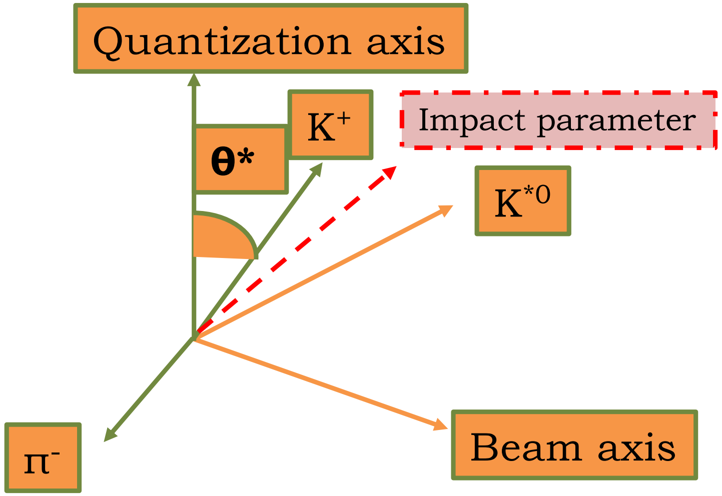

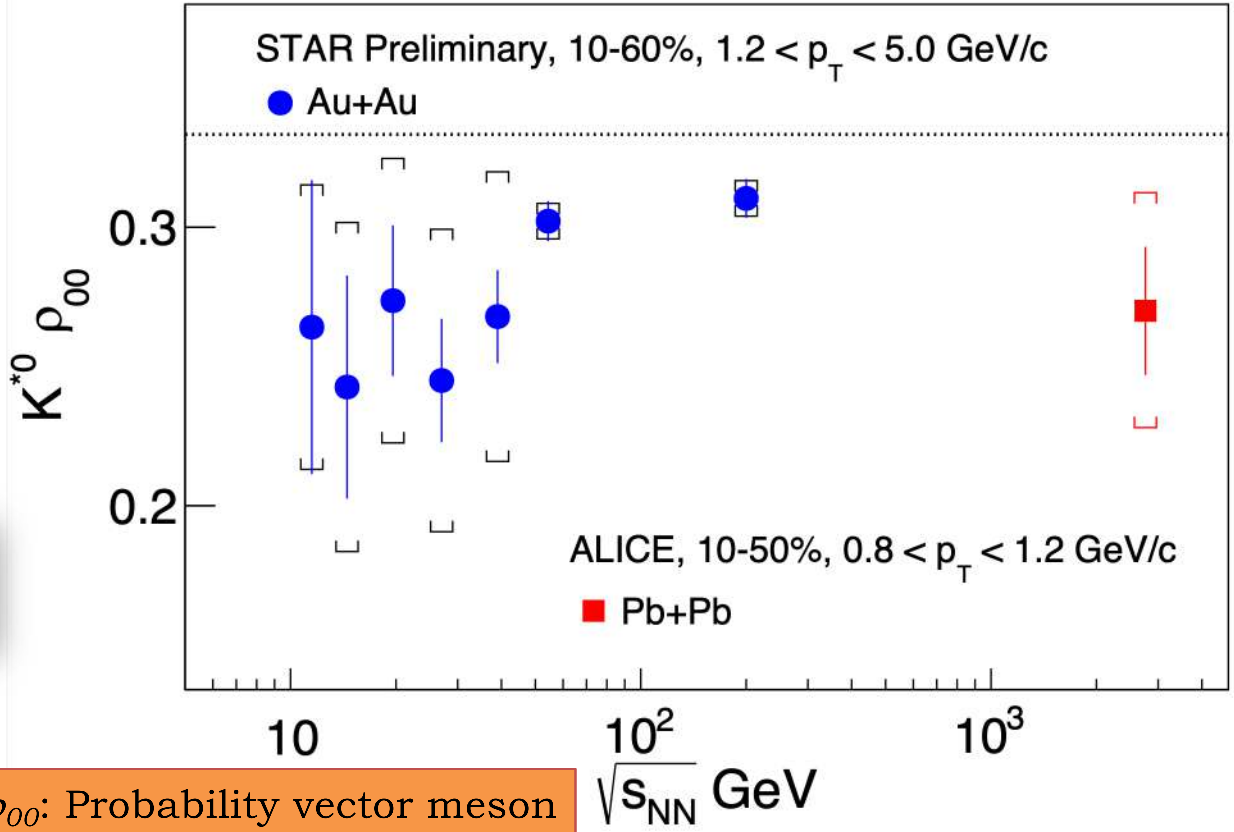

$$\frac{dN}{dcos\theta} = N_0\left[1 - \rho_{0,0} + cos^2\theta\,(3\rho_{0,0} - 1)\right]$$

$\rho_{00} = 1/3$ → No spin alignment

STAR: QM2019
ALICE: Phys. Rev. Lett. 125, 012301 (2020)

ρ_{00}: Probability vector meson is in spin state = 0

- ✓ Evidence of spin alignment in vector mesons in high energy **heavy-ion collisions**.
- ✓ Measurement **coupled to** Event Plane – related to **initial angular momentum**

Chirality related (conclusions)

The charge separation along the magnetic field observed. Measurements could be related to **chiral magnetic effect.**

The Δv_2 (π^+ - π^-) vs. ch. particle number asymmetry of the event observed. Measurements could be related to **chiral magnetic wave.**

Polarization of Lambda baryons observed in RHIC-BES energies. **Spin alignment of vector mesons** observed in RHIC BES and LHC energies. Measurements could be related to the **spin-orbital angular momentum interactions.**

These measurements leads to new theoretical developments.
-- Relativistic spin and magneto hydrodynamics)

20 years of pushing the tests of QCD at high temperature and density to limits …

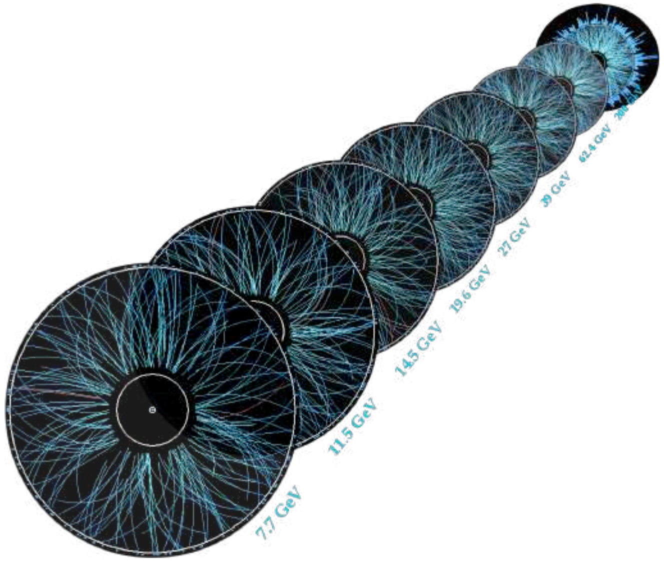

Overall conclusions

Thermalization
QGP
EOS
CP
$\vec{L}\cdot\vec{S}$ and $\vec{\mu}\cdot\vec{B}$
η/s ….

Non-monotonic variations (BES)

Mean transverse mass/energy

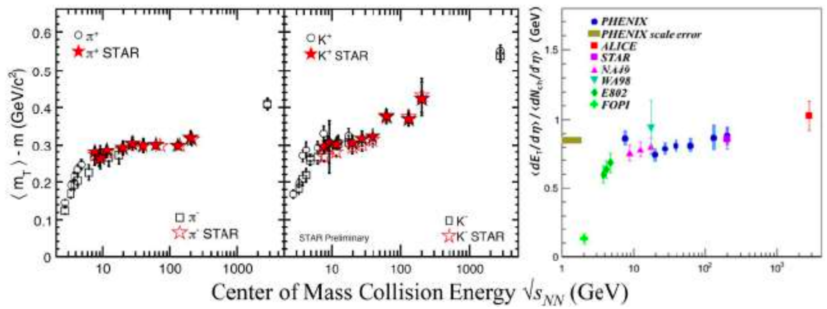

v$_3$ fluctuations

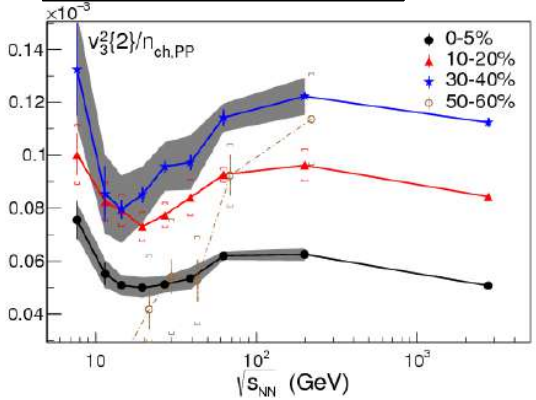

Net-proton v$_1$ slope

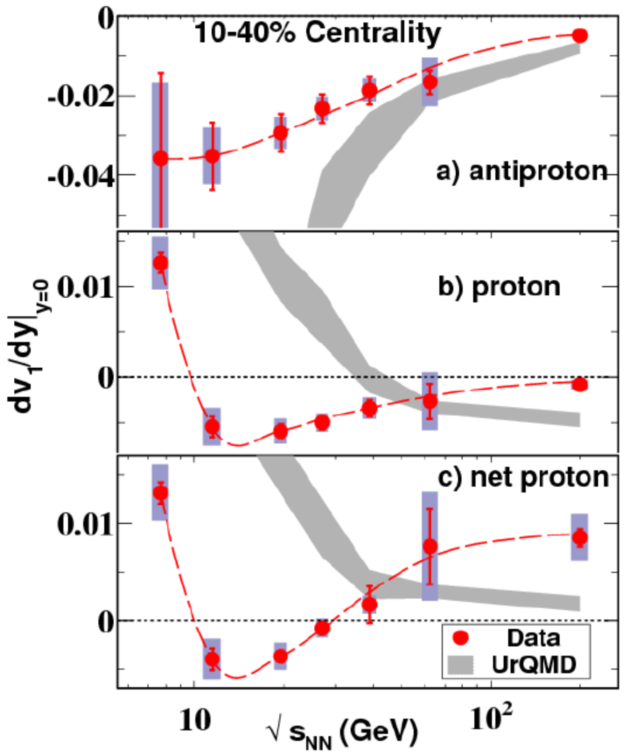

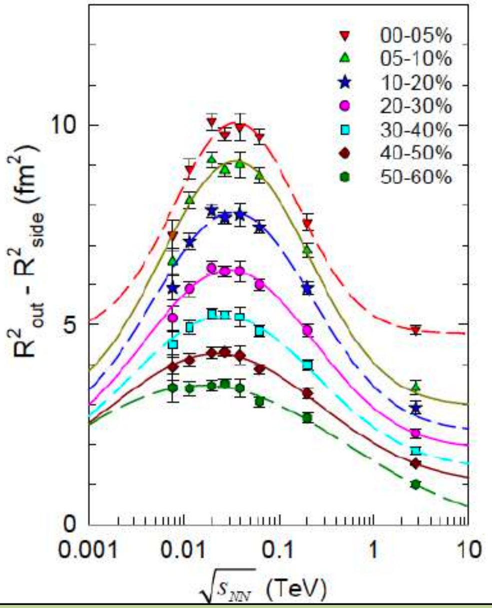

HBT Radii, *Phys. Rev. Lett. 114, 142301 (2015)*

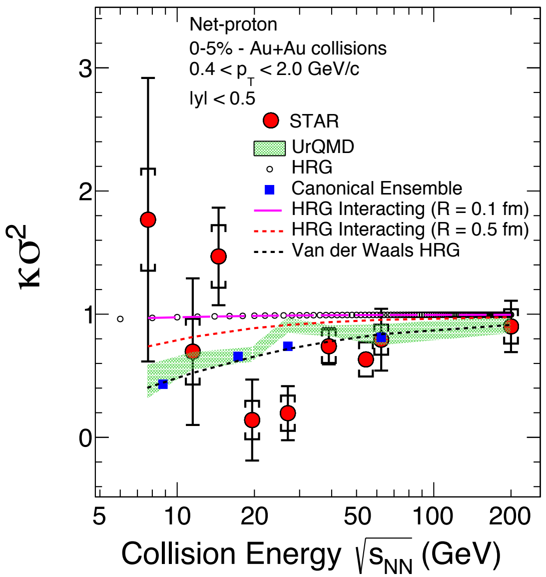

Net-proton fluctuations

Turn-off of QGP like features (BES)

Nuclear modification factor

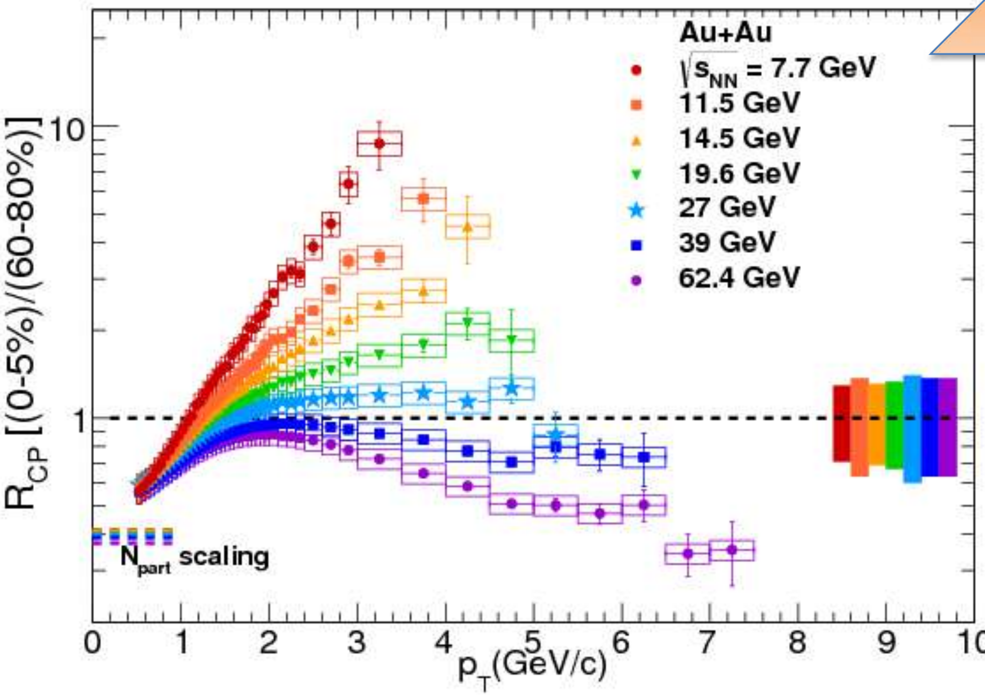

STAR: Phys.Rev.Lett. 121 (2018) 3, 032301
STAR: Phys.Rev.Lett. 110 (2013) 14, 142301

High-p_T net suppression to net enhancement

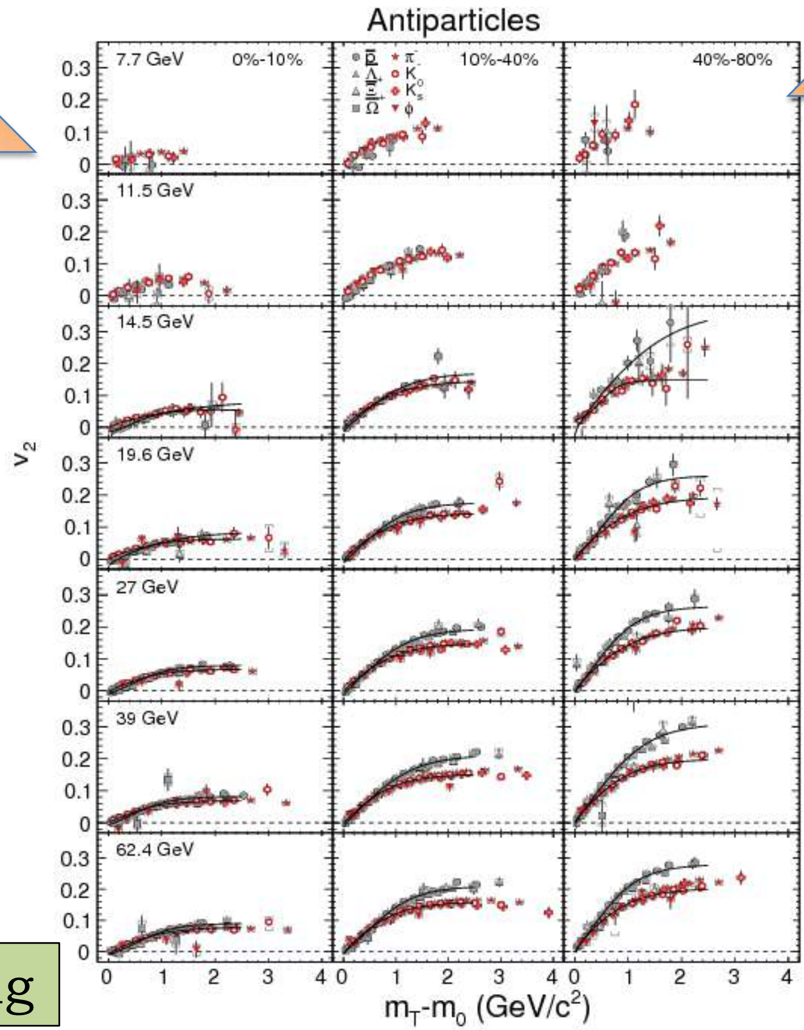

Turn off NCQ scaling

Partonic collectivity, NCQ scaling

Properties of the system (role of BES)

Quantity	~ Value	Reference
Initial temperature	300 – 600 MeV (high energy)	Phys.Rev.Lett. 104 (2010) 132301
Chemical freeze-out temperature	168 (high energy) – 144 MeV (low energy)	*Phys.Rev.C* 96 (2017) 4, 044904
Baryonic chemical potential	18 (high energy) – 398 MeV (low energy)	
Strangeness supp. factor (γ_s)	0.5 (low energy) – 1.0 (high energy)	
Kinetic Freeze-out Temperature	113 (high energy) -143 (low energy) MeV	
Radial Collective Velocity	0.1 – 0.5 c	
Homogenous volume (HBT)	1900 (low energy) – 2800 fm^3 (high energy)	Phys.Rev.C 92 (2015) 1, 014904
System lifetime (HBT)	4 (low energy) – 7 fm/c (high energy)	
Shear viscosity/entropy (η/s) Stopping power ($\hat{q}$) Diffusion co-efficient (D x $2\pi T$)	0.08 (high energy) – 0.2 (low energy) 2-10 GeV^2/fm (high energy) 1 - 10 (high energy)	Phys. Rev. C 91, 064901 (2015) Phys.Rev.C 97 (2018) 4, 044905
Vorticity (average)	$(9\pm1)\times10^{21} s^{-1}$	Nature 548 (2017) 62

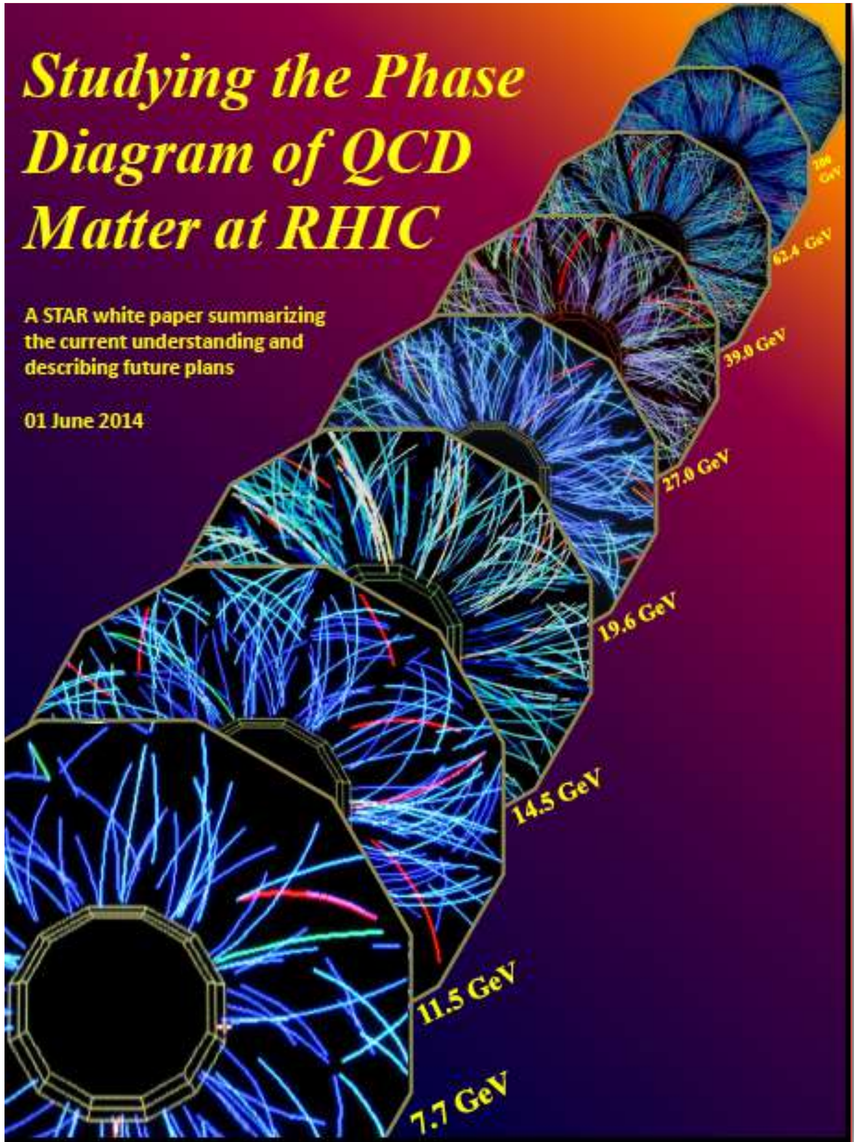

BES-II and FXT

1) The inner TPC (iTPC) to extend the coverage to $|\eta| < 1.5$, p_T acceptance down to 100 MeV/c and better dE/dx resolution.
2) The endcap TOF (eTOF) detector will extend the particle identification capability to $-1.6 < \eta < 1.0$.
3) The Event Plane Detector (EPD) at $2.1 < |\eta| < 5.1$ will allow centrality selection and event plane measurements.

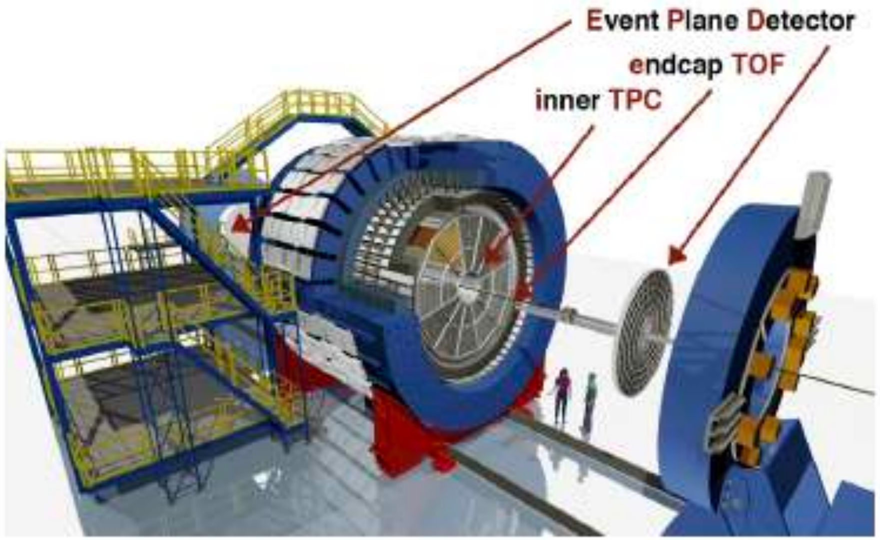

2019 - 2021: BES-II at RHIC

$\sqrt{s_{NN}}$ (GeV)	Events (10^6)	BES II / BES I	Weeks	μ_B (MeV)	T_{CH} (MeV)
200	350	2010		25	166
62.4	67	2010		73	165
54.4	1200	2017		90	
39	39	2010		112	164
27	70	2011		156	162
19.6	**400** / 36	**2019-21** / 2011	**3**	206	160
14.5	**300** / 20	**2019-21** / 2014	**2.5**	264	156
11.5	**230** / 12	**2019-21** / 2010	**5**	315	152
9.2	**160** / 0.3	**2019-21** / 2008	**9.5**	355	140
7.7	**100** / 4	**2019-21** / 2010	**14**	420	140

Precision measurements: map the QCD phase diagram **$200 < \mu_B < 420$MeV.**

RHIC – Fixed Target Program

Collider Energy	Fixed-Target Energy	Single beam AGeV	Center-of-mass Rapidity	μ_B (MeV)
62.4	7.7	30.3	2.10	420
39	6.2	18.6	1.87	487
27	5.2	12.6	1.68	541
19.6	4.5	8.9	1.52	589
14.5	3.9	6.3	1.37	633
11.5	3.5	4.8	1.25	666
9.1	3.2	3.6	1.13	699
7.7	3.0	2.9	1.05	721
5.0	2.5	1.6	0.82	774

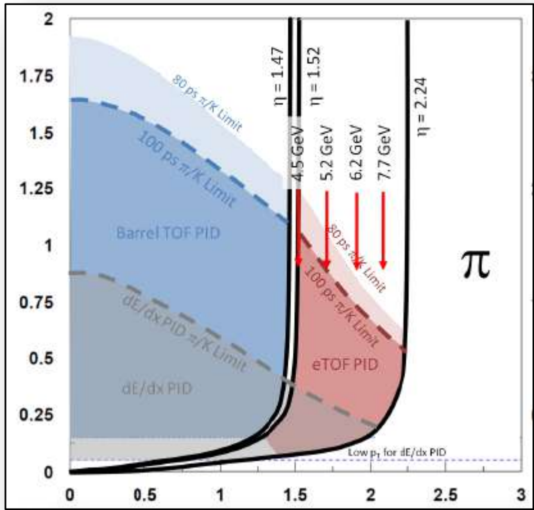

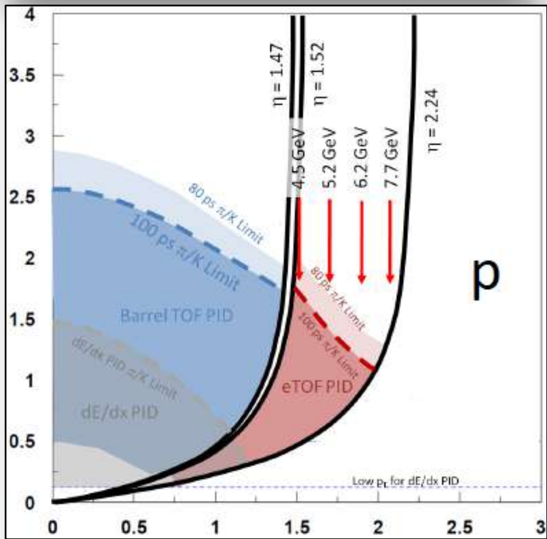

D. Cebra: INT Program INT-16-3: Exploring the QCD Phase Diagram through Energy Scans. **Extend scan to 750 MeV in μ_B.**

RHIC BES program

1. Systematic study of the phase structure of QCD Phase diagram.

2. Opportunity for a dedicated study of high baryon density matter
   a) Finding direct signals of true phase transition and critical point.
   b) Understanding the properties of high baryon density, rotating QCD matter under magnetic field.
   c) Understanding nuclei, hyper-nuclei and exotic nuclei formation and properties.

3. Complementary to research programs at CERN, FAIR & NICA.

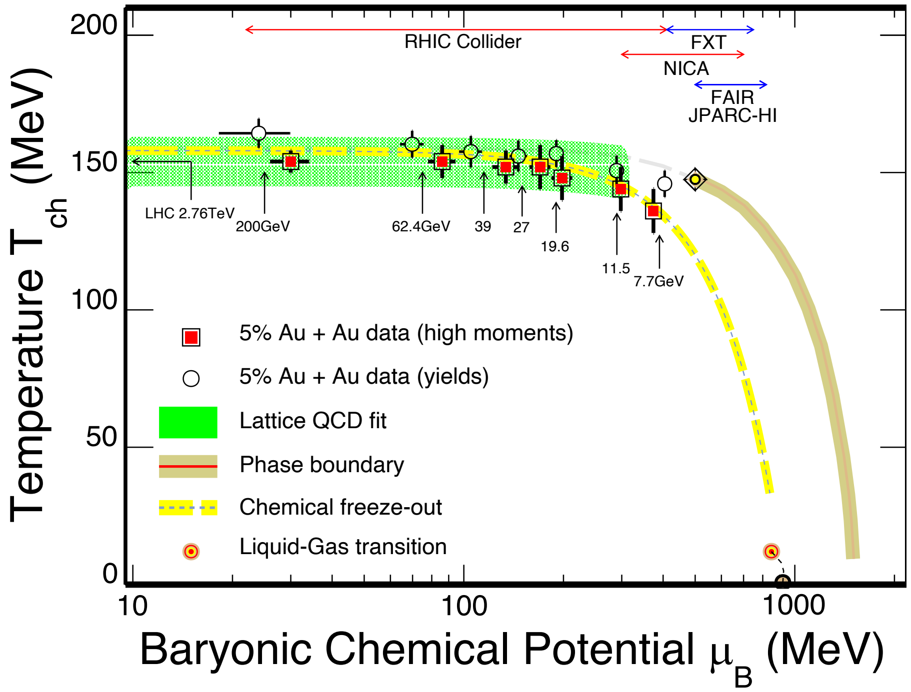

e-Print: 2004.04681 [hep-ph]

25+ Publications: 8 PRL and 1 Nature

RHIC BES

Chemical freeze-out properties
- T
- μ_B, μ_S, μ_Q
- γ_s

Collectivity
- EOS: Partonic vs. Hadronic
- Shear viscosity
- Diffusion
- Nature of transition

Chirality
- CME, CVE, CMW
- Polarization

Criticality

Exotic nuclei and high baryon density matter

QGP

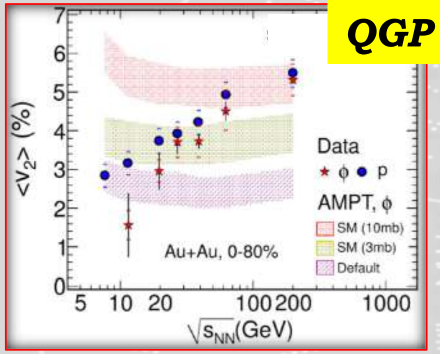

CP

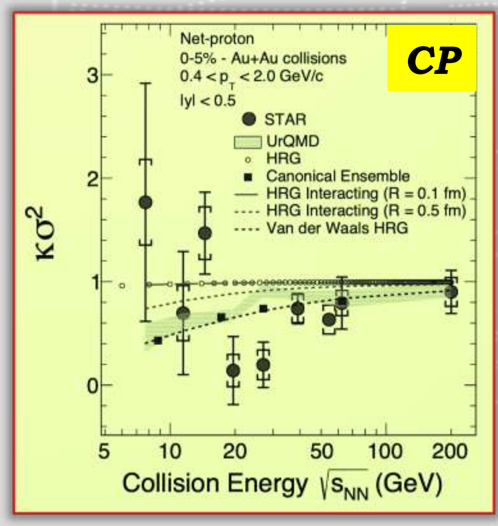

Thermal

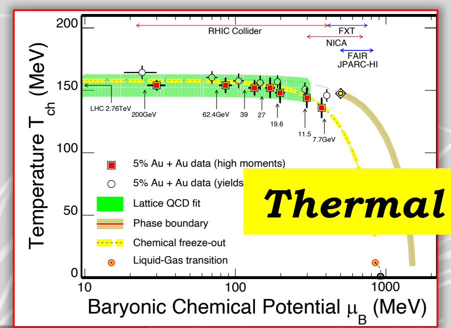

EOS

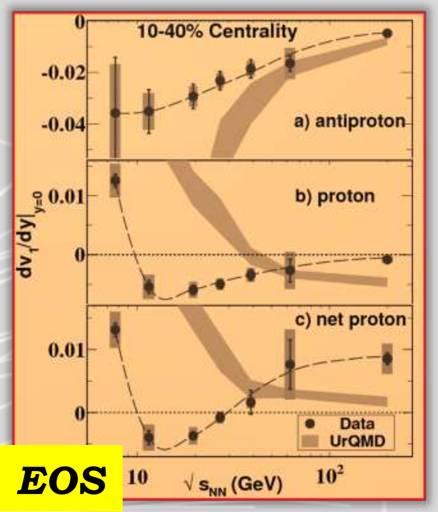

$\vec{L} \cdot \vec{S}$

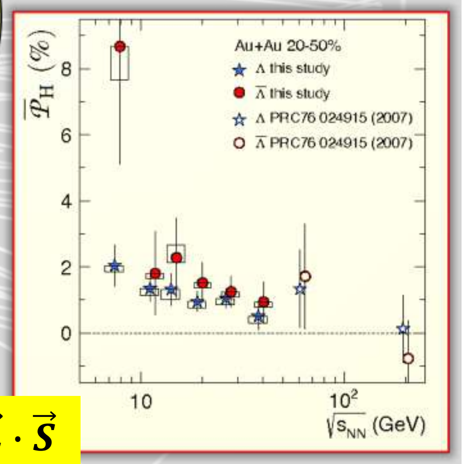

Acknowledgements

Thanks to the Organizers, particularly : Huichao Song, Ulrich Heinz and Nu Xu

Thanks to all STAR Collaborators